Few Fixed Variants between Trophic Specialist Pupfish Species Reveal Candidate *Cis*-Regulatory Alleles Underlying Rapid Craniofacial Divergence

Joseph A. McGirr[1] and Christopher H. Martin *[,2]

[1]Environmental Toxicology Department, University of California, Davis, CA

[2]Department of Integrative Biology and Museum of Vertebrate Zoology, University of California, Berkeley, CA

***Corresponding author:** E-mail: chmartin@berkeley.edu.

Associate editor: Patricia Wittkopp

Abstract

Investigating closely related species that rapidly evolved divergent feeding morphology is a powerful approach to identify genetic variation underlying variation in complex traits. This can also lead to the discovery of novel candidate genes influencing natural and clinical variation in human craniofacial phenotypes. We combined whole-genome resequencing of 258 individuals with 50 transcriptomes to identify candidate *cis*-acting genetic variation underlying rapidly evolving craniofacial phenotypes within an adaptive radiation of *Cyprinodon* pupfishes. This radiation consists of a dietary generalist species and two derived trophic niche specialists—a molluscivore and a scale-eating species. Despite extensive morphological divergence, these species only diverged 10 kya and produce fertile hybrids in the laboratory. Out of 9.3 million genome-wide SNPs and 80,012 structural variants, we found very few alleles fixed between species—only 157 SNPs and 87 deletions. Comparing gene expression across 38 purebred F1 offspring sampled at three early developmental stages, we identified 17 fixed variants within 10 kb of 12 genes that were highly differentially expressed between species. By measuring allele-specific expression in F1 hybrids from multiple crosses, we found that the majority of expression divergence between species was explained by *trans*-regulatory mechanisms. We also found strong evidence for two *cis*-regulatory alleles affecting expression divergence of two genes with putative effects on skeletal development (*dync2li1* and *pycr3*). These results suggest that SNPs and structural variants contribute to the evolution of novel traits and highlight the utility of the San Salvador Island pupfish system as an evolutionary model for craniofacial development.

Key words: **RNAseq, F1 hybrid, trophic specialization, allele-specific expression, adaptive radiation, ecological speciation.**

Article

Introduction

Developing a mechanistic understanding of genetic variation contributing to variation in complex craniofacial traits is a major goal of both basic and translational research. This involves identifying genetic variants influencing natural morphological diversity as well as craniofacial anomalies, which account for approximately one-third of all birth defects (Gorlin et al. 1990). It is now understood that much of the natural and clinical variation in complex traits like craniofacial morphology results from interactions among hundreds to thousands of loci across the genome (Boyle et al. 2017; Sella and Barton 2019). Genome-wide association studies (GWAS) have shown that the vast majority of genetic variants affecting complex traits and diseases are within noncoding regions, highlighting the importance of gene regulation influencing trait variation (Hindorff et al. 2009; Maurano et al. 2012; Schaub et al. 2012). However, much of what is currently known about the developmental genetic basis of craniofacial diversity comes from mutagenesis screens and loss of function experiments in model organisms. These types of experiments are biased to detect alleles within protein-coding regions that severely disrupt gene function and are likely to cause lethality at early developmental stages (Nguyen and Xu 2008; Hall 2009). Thus, complementary approaches to mutagenesis screens are necessary to identify genes that influence craniofacial phenotypes at later stages in development though changes in gene regulation rather than gene function.

One such approach is to harness naturally occurring genetic variation between "evolutionary mutants"—closely related species exhibiting divergent phenotypes that mimic human disease phenotypes (Albertson et al. 2008). Several fish systems have been particularly useful as models for craniofacial developmental disorders because closely related species are often distinguished by differences in morphological traits important for trophic niche specialization, such as the shape and dynamics of jaws and pharyngeal elements (Albertson et al. 2008; Schartl 2014; Powder and Albertson 2016). The process of identifying candidate genes and validating their effect on phenotypic divergence in evolutionary

mutants typically involves population genomic analyses, gene expression analyses, GWAS, and functional validation experiments (Bono et al. 2015; Kratochwil and Meyer 2015). Using a combination of these approaches, research in fish systems has shown that the evolution of adaptive craniofacial traits often involve orthologs of genes implicated in human disorders (Albertson et al. 2005; Helms et al. 2005; Roberts et al. 2011; Ahi et al. 2014; Cleves et al. 2014; Lencer et al. 2017; Erickson et al. 2018; Gross and Powers 2018; Martin et al. 2019). Therefore, candidate genes identified in evolutionary mutant models that have orthologs with uncharacterized functions in humans warrant further study into their relationship with development and disease.

Measuring relative and absolute genetic differentiation (estimated as *Fst* and *Dxy*) between species can reveal diverged regions of the genome that may influence trait development, but these statistics alone are insufficient to identify genetic mechanisms underlying evolutionary mutant phenotypes (Nachman and Payseur 2012; Cruickshank and Hahn 2014). RNA sequencing across multiple developmental stages and tissue types can provide further evidence that differentiated regions influence phenotypic divergence if genes near genetic variants are differentially expressed between species (Bernatchez et al. 2010; Poelstra et al. 2014; McGirr and Martin 2018; Verta and Jones 2019). However, this assumes that linked genetic variation within *cis*-acting regulatory elements affects proximal gene expression levels, and does not rule out the possibility of unlinked *trans*-acting regulatory variation binding regulatory regions to influence expression levels (Wittkopp and Kalay 2012; Signor and Nuzhdin 2018).

It is possible to use RNAseq to identify mechanisms of gene expression divergence between parental species by bringing *cis* elements from both parents together in the same *trans* environment in F1 hybrids and quantifying allele-specific expression (ASE) of parental alleles at heterozygous sites (Cowles et al. 2002; Wittkopp et al. 2004; Signor and Nuzhdin 2018). Determining whether a candidate gene is differentially expressed due to *cis*- or *trans*-regulatory divergence is important to identify putatively causal alleles that can be further validated by genome editing or transgenesis experiments. Furthermore, this type of analysis can reveal the relative contribution of *cis*- and *trans*- variation influencing genome-wide patterns of expression divergence. Some studies have found a larger contribution of *cis*-regulatory variation underlying expression divergence between species (Graze et al. 2009; Shi et al. 2012; Schaefke et al. 2013; Davidson and Balakrishnan 2016; Mack and Nachman 2017), whereas others have shown expression patterns dominated by *trans*-acting variation (Streisfeld and Rausher 2009; McManus et al. 2010; Hart et al. 2018). Overall, *cis*-acting alleles are generally thought to contribute more to interspecific divergence and show mostly additive inheritance, while *trans*-acting alleles are often more pleiotropic, contribute more to intraspecific divergence, and show nonadditive inheritance (Prud'homme et al. 2007; Lemos et al. 2008; Signor and Nuzhdin 2018).

Here, we combine whole-genome resequencing, RNAseq, and F1 hybrid ASE analyses to identify regulatory mechanisms influencing rapidly evolving craniofacial phenotypes within an adaptive radiation of *Cyprinodon* pupfishes on San Salvador Island, Bahamas (fig. 1). This sympatric radiation consists of a dietary generalist species (*C. variegatus*) and two endemic specialist species adapted to novel trophic niches—a molluscivore (*C. brontotheroides*) and a scale-eater (*C. desquamator*; Martin and Wainwright 2013a). Nearly all 49 pupfish species in the genus *Cyprinodon* distributed across North America and the Caribbean are dietary generalists with similar craniofacial morphology that is used for consuming algae and small invertebrates (fig. 1A; Martin and Wainwright 2011, 2013b). The molluscivore evolved short, thick oral jaws stabilized by a nearly immobile maxilla allowing it to specialize on hard-shelled prey including ostracods and gastropods (fig. 1B). This morphology results in a larger in-lever to out-lever ratio compared with generalists, increasing mechanical advantage for strong biting (Hernandez et al. 2018). The molluscivore is also characterized by a prominent maxillary anteriodorsal protrusion that may be used as a wedge for extracting snails from their shells (Martin et al. 2017; St. John et al. 2020a). The scale-eater is a predator that evolved to bite scales and protein-rich mucus removed from other pupfish species during rapid feeding strikes (fig. 1C; St. John et al. 2020b). Scale-eaters have greatly enlarged oral jaws, larger adductor mandibulae muscles, darker breeding coloration, and a more elongated body compared with the generalist and molluscivore species (Martin and Wainwright 2013a).

Exceptional craniofacial divergence despite extremely recent divergence times and low genetic differentiation between molluscivores and scale-eaters make this system a compelling evolutionary model for human craniofacial developmental disorders. These trophic specialist species rapidly diverged from an ancestral generalist phenotype within the last 10–15 k years (Turner et al. 2008; Martin and Feinstein 2014). Molluscivores and scale-eaters readily hybridize in the laboratory to produce fertile F1 offspring with approximately intermediate craniofacial phenotypes between the parents and no obvious sex ratio distortion (Martin and Wainwright 2013b; Martin and Feinstein 2014). These species show evidence of premating isolation in the laboratory (West and Kodric-Brown 2015) and are genetically differentiated in sympatry (genome-wide mean $Fst = 0.14$ across 12 million SNPs; McGirr and Martin 2017).

We previously identified 31 genomic regions (20 kb) that contained SNPs fixed between species ($Fst = 1$), showed signs of a hard selective sweep, and were significantly associated with oral jaw size using multiple genome-wide association mapping approaches (McGirr and Martin 2017). A subset of these fixed SNPs fell within significant QTL explaining 15% of variation in oral jaw size and were near genes annotated for effects on skeletal system development (Martin et al. 2017). Here, we use complementary approaches to identify candidate causal variants putatively influencing craniofacial divergence by 1) incorporating transcriptomic data from 122 individuals sampled at three developmental stages (McGirr and Martin 2018, 2019), 2) applying genome divergence scans to a much larger sample of whole genomes from San Salvador Island and surrounding Caribbean outgroup populations (increasing $n = 37–258$) aligned to a new high-quality de novo

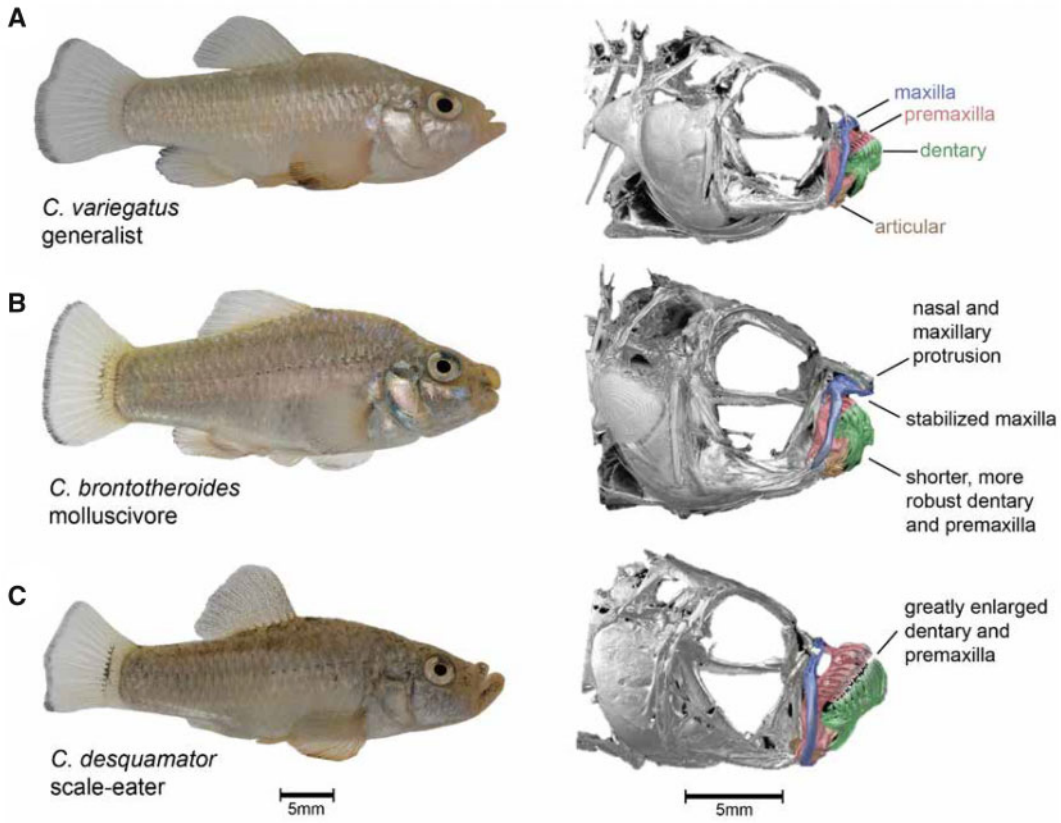

FIG. 1. San Salvador Island pupfishes exhibit exceptional craniofacial divergence despite recent divergence times. (*A*) *Cyprinodon variegatus* (generalist), (*B*) *C. brontotheroides* (molluscivore), (*C*) *C. desquamator* (scale-eater). µCT scans modified from (Hernandez et al. 2018) show major craniofacial skeletal structures diverged among species including the maxilla (blue), premaxilla (red), dentary (green), and articular (brown).

genome assembly (Richards et al. 2020), 3) identifying structural variation fixed between species for the first time in this system, and 4) inferring *cis*- and *trans*-regulatory mechanisms underlying gene expression divergence between species using 12 F1 hybrid transcriptomes. Overall, we found that *trans*-regulatory divergence was responsible for more expression divergence between species than *cis*-regulatory mechanisms. We also identified two genes showing *cis*-regulatory divergence that were near just one fixed variant each: a deletion upstream of a gene known to influence skeletal development (*dync2li1*) and a SNP downstream of a novel skeletal candidate gene (*pycr3*). Our results highlight the utility of using these closely related species replicated across isolated lake populations as an evolutionary model for craniofacial development and provide highly promising candidate variants for future functional validation experiments.

Results

Few Fixed Variants between Young Species Showing Drastic Craniofacial Divergence

We analyzed whole-genome resequencing samples for 258 *Cyprinodon* pupfishes (median coverage = 8×; Richards et al. 2020). This included 114 individuals from multiple isolated lake populations on San Salvador Island (33 generalists, 46 molluscivores, and 35 scale-eaters) and 140 outgroup generalist pupfishes from across the Caribbean and North America. Libraries for 150PE Illumina sequencing were generated from DNA extracted from muscle tissue and the resulting reads were mapped to the *C. brontotheroides* reference genome (v 1.0; total sequence length = 1,162,855,435 bp; number of scaffolds = 15,698, scaffold N50, = 32,000,000 bp; L50 = 15 scaffolds; Richards et al. 2020). Variants were called using the Genome Analysis Toolkit (GATK v 3.5; DePristo et al. 2011) and filtered to include SNPs with a minor allele frequency above 0.05, genotype quality above 20, and sites with greater than 50% genotyping rate across all individuals.

Out of 9.3 million SNPs identified in our data set, we found a mere 157 SNPs fixed between molluscivore and scale-eater specialist species showing $Fst = 1$ (fig. 2A; mean genome-wide $Fst = 0.076$). Of these 157 variants, 46 were within 10 kb of 27 genes and none were in coding regions. These 27 genes were enriched for 27 biological processes ($P < 0.05$), including several ontologies describing neuronal development and activity of cell types within bone marrow (fig. 2B and supplementary table S1, Supplementary Material online).

Structural variants (including insertions, deletions, inversions, translocations, and copy number variants) have been traditionally difficult to detect in nonmodel systems and ignored by many early whole-genome comparative studies (Stapley et al. 2010; Ho et al. 2019; Wellenreuther et al. 2019). We identified 80,012 structural variants across eight molluscivore and scale-eater individuals using a method that

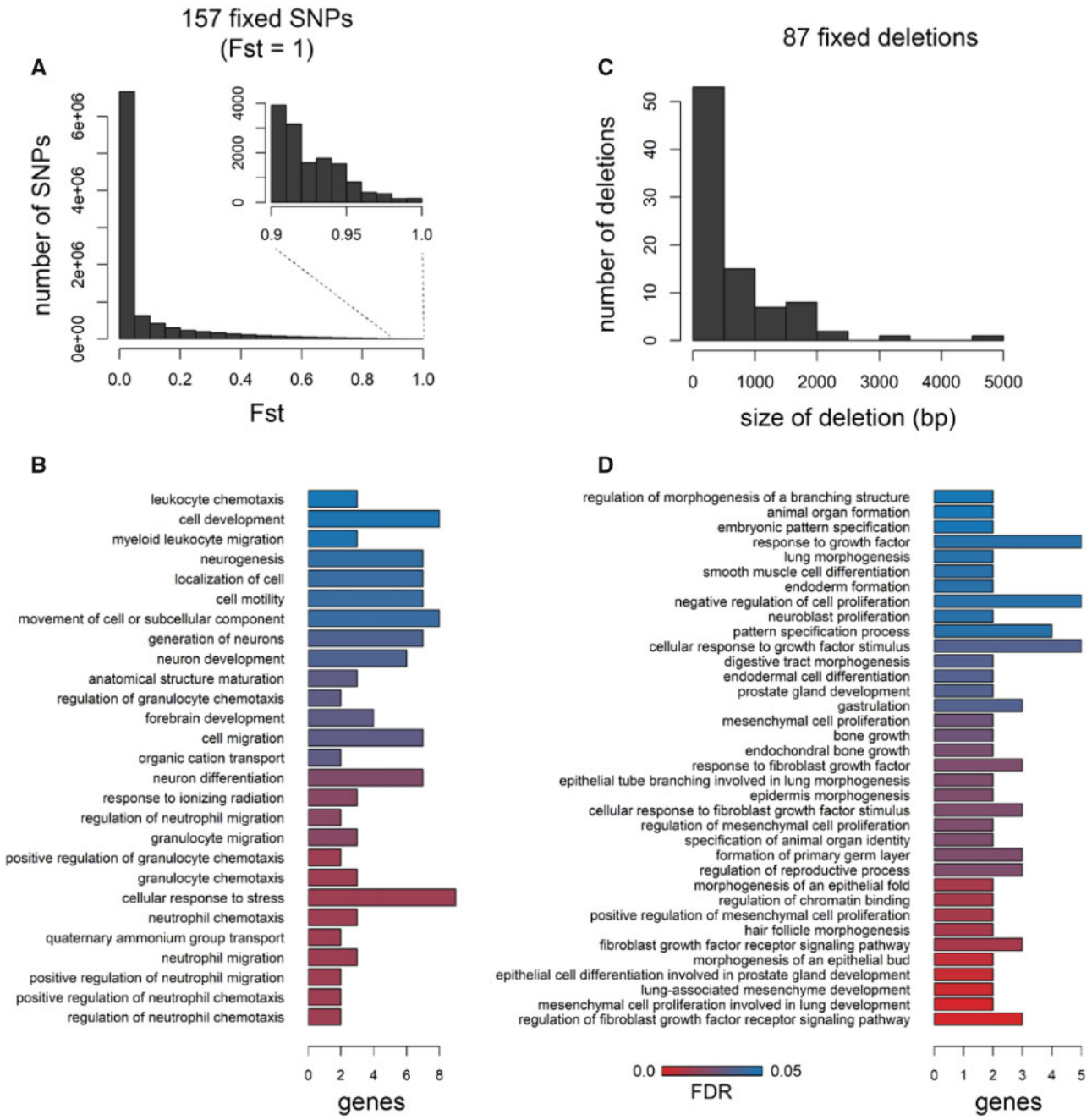

FIG. 2. Very few SNPs and structural variants are fixed between trophic specialists. (*A*) Distribution of Weir and Cockerham *Fst* values across 9.3 million SNPs; 157 were fixed between species ($Fst = 1$). (*B*) Forty-six of the 157 SNPs were located near 27 genes that were enriched for 27 biological processes (FDR < 0.05). (*C*) Size distribution of the 87 deletions is fixed between species out of 80,012 structural variants. (*D*) Thirty-four of the 87 fixed deletions were within 10 kb of 34 genes that were enriched for 36 biological processes.

calls variants based on combined evidence from paired-end clustering and split read analysis (Rausch et al. 2012). Just 87 structural variants were fixed between species and, strikingly, all structural variants were deletions fixed in scale-eaters. This may reflect differences in the position of fitness optima between scale-eaters and molluscivores relative to the putative ancestral optimum. We expect larger effect mutations, such as deletions, to be more likely to fix in scale-eaters than molluscivores due to the more distant position of the fitness optimum for scale-eating (Martin et al. 2017). Differences in population size may also explain why all deletions are fixed in scale-eaters, which have a smaller effective population size than molluscivores (Richards and Martin 2017; Richards et al. 2020). These deletions ranged in size between 55 and 4,703 bp (fig. 2*C*). Of these, 34 fixed deletions were near 34 genes (supplementary table S1, Supplementary Material online). Only a single fixed deletion (1,256 bp) was found within a protein coding region, spanning the entire fifth exon of *gpa33* (fig. 3). The 34 genes near fixed deletions were enriched for 36 biological processes ($P < 0.05$), including ontologies describing bone development, mesenchyme development, fibroblast growth, and digestive tract development (fig. 2*D*).

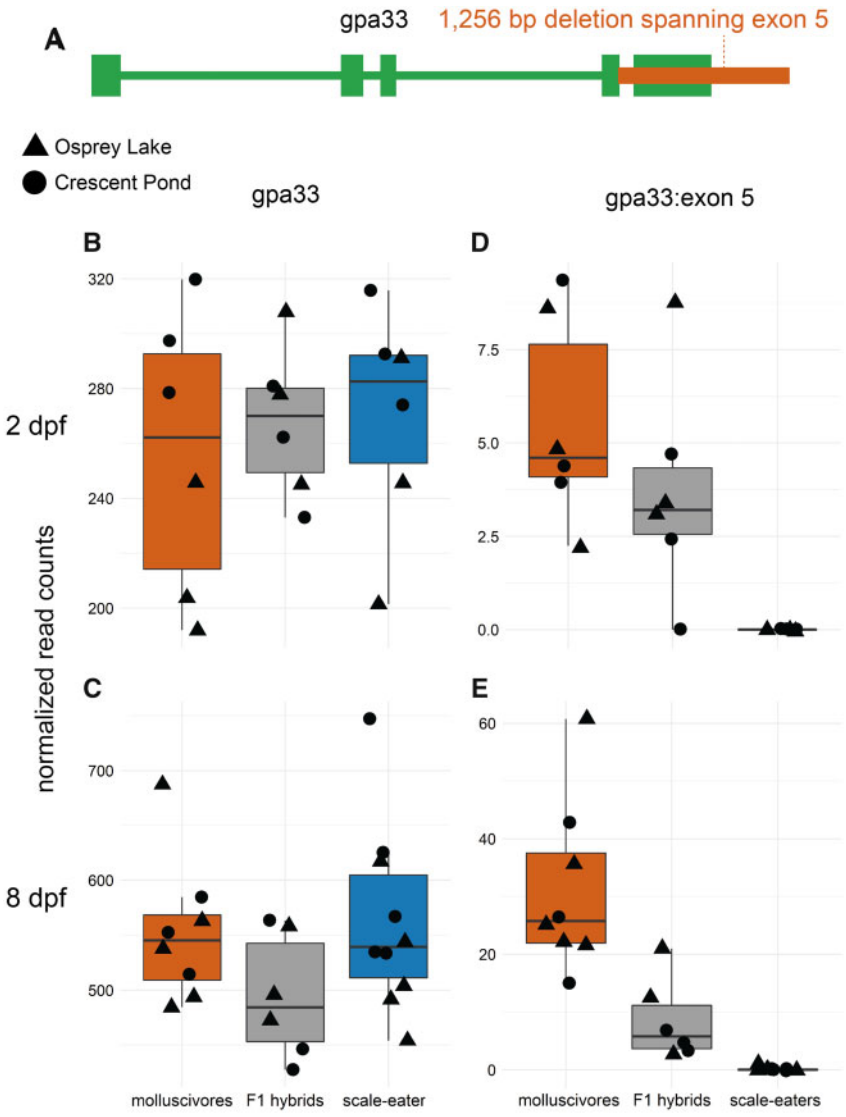

Fig. 3. The only fixed variant within a protein coding region is an exon deletion of *gpa33*. (*A*) A 1,256 bp deletion (red) identified by DELLY spans the entire fifth exon of *gpa33* and is fixed in scale-eaters. (*B* and *C*) The gene is not significantly differentially expressed between molluscivores (red) and scale-eaters (blue) at 2 or 8 dpf when considering read counts across all exons ($P > 0.05$). (*D* and *E*) However, when only considering the fifth exon, scale-eaters show no expression and F1 hybrids (gray) show reduced expression, supporting evidence for the deletion.

Including SNPs and deletions, we found a total of 80 fixed variants within 10 kb of 59 genes (supplementary table S1, Supplementary Material online). Encouragingly, 41 of these genes (70%) also showed high between population nucleotide divergence ($Dxy > 0.0083$; genome-wide 90th percentile), strengthening evidence for adaptive divergence at these loci. Variants with larger effect sizes are predicted to fix faster than variants with smaller effects (Griswold 2006; Yeaman and Whitlock 2011; Stetter et al. 2018). However, there are likely many alleles contributing to craniofacial divergence that are segregating between populations of molluscivores and scale-eaters. We also identified genes near SNPs showing lower values of *Fst* that were still highly differentiated between species ($Fst > 0.72$; genome-wide 99th percentile and $Dxy > 0.0083$; genome-wide 90th percentile) and within 20 kb of a gene. Using these thresholds, we found 63,542 SNPs near 1,940 genes. This gene set was enriched for 420 biological processes ($P < 0.01$), including embryonic cranial skeleton morphogenesis, bone mineralization, muscle structure development, and forebrain development (supplementary table S2, Supplementary Material online).

Genes near Fixed Variants Are Differentially Expressed throughout Development

All but 1 of the 80 variants fixed between species were in noncoding regions, suggesting that these variants may affect species-specific phenotypes through regulation of nearby genes. To identify patterns of gene expression divergence between species, we combined two previous transcriptomic data sets spanning three developmental stages and three San Salvador Island lake populations (McGirr and Martin 2018, 2019). F1 offspring were sampled at 2, 8, and 20 days

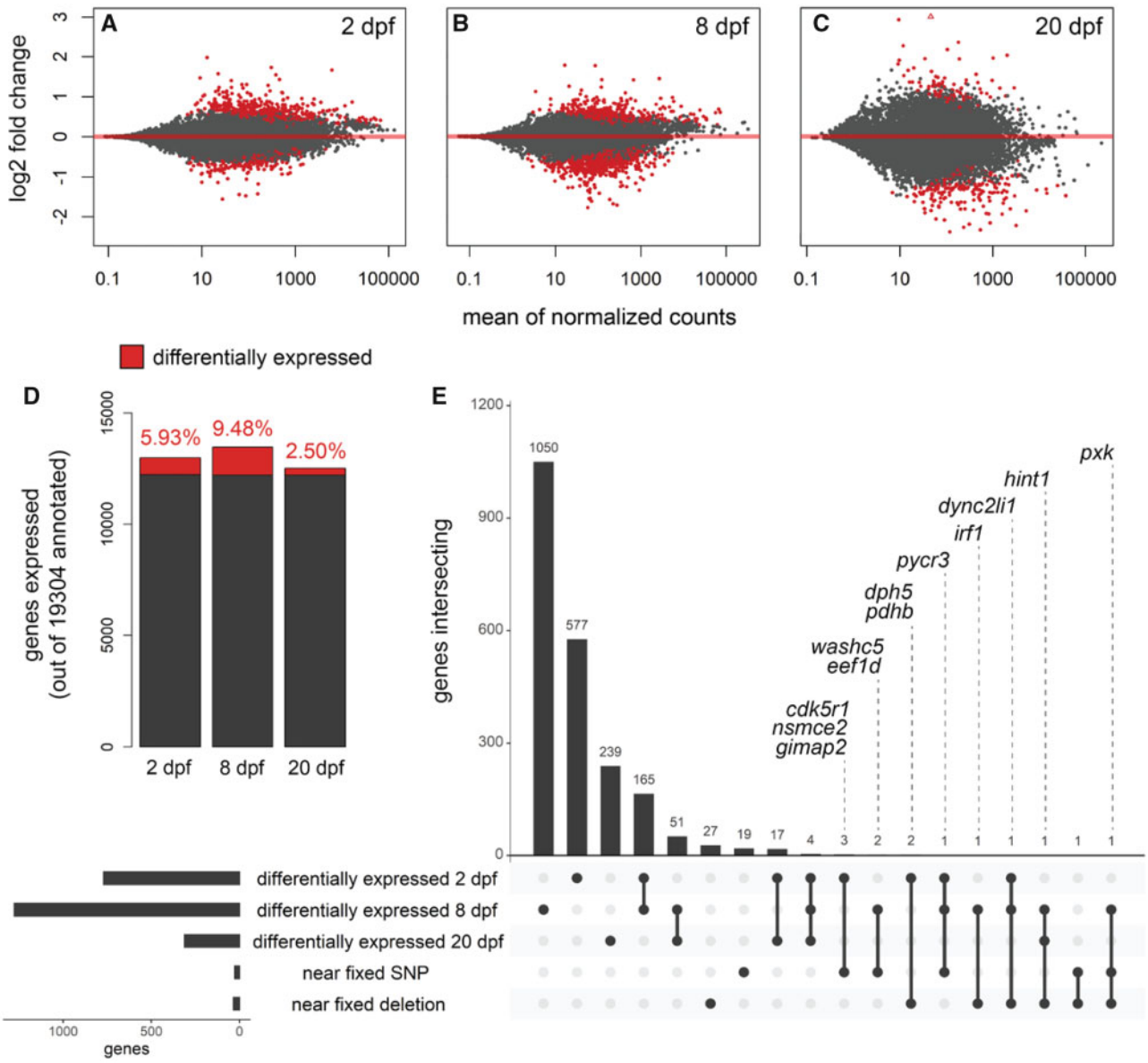

Fig. 4. Genes near fixed variants are differentially expressed between species across three developmental stages. Genes differentially expressed (red; $P < 0.01$) between molluscivores and scale-eaters at (*A*) 2dpf, (*B*) 8 dpf, and (*C*) 20 dpf. Positive log2 fold changes indicate higher expression in scale-eaters relative to molluscivores. (*D*) Proportion of genes differentially expressed out of the total number of genes expressed across three stages. (*E*) UpSet plot (Conway et al. 2017) showing intersection across five sets: genes differentially expressed at each of the three stages, genes within 10 kb of fixed SNPs, and genes within 10 kb of fixed deletions. The 12 labeled genes were differentially expressed during at least one stage and within 10 kb of fixed variants.

postfertilization (dpf). RNA was extracted from whole body tissue at 2 and 8 dpf; whereas 20 dpf samples were dissected to only extract RNA from craniofacial tissues (supplementary table S3, Supplementary Material online). The earlier developmental stages are described as stage 23 (2 dpf) and 34 (8 dpf) in a recent embryonic staging series of *C. variegatus* (Lencer and McCune 2018). The 2 dpf stage is comparable with the Early Pharyngula Period of zebrafish, when multipotent neural crest cells have begun migrating to pharyngeal arches that will form the oral jaws and most other craniofacial structures (Schilling and Kimmel 1994; Furutani-Seiki and Wittbrodt 2004; Lencer et al. 2017). Embryos usually hatch 6–10 dpf, with similar variation in hatch times among species (Lencer et al. 2017; McGirr and Martin 2018). While some cranial elements are ossified prior to hatching, the skull is largely cartilaginous at 8 dpf and ossified by 20 dpf (Lencer and McCune 2018).

We used DEseq2 (Love et al. 2014) to contrast gene expression in pairwise comparisons between species grouped by developmental stage (sample sizes for comparisons [molluscivores vs. scale-eaters]: 2 dpf = 6 vs. 6, 8 dpf = 8 vs. 10, 20 dpf = 6 vs. 2). Out of 19,304 genes annotated for the *C. brontotheroides* reference genome, we found 770 (5.93%) significantly differentially expressed at 2 dpf, 1,277 (9.48%) at 8 dpf, and 312 (2.50%) at 20 dpf (fig. 4*A*–*D*). The lower number of genes differentially expressed at 20 dpf likely reflects

Table 1. Twelve Genes Differentially Expressed between Molluscivores and Scale-Eaters at 2 , 8, and/or 20 dpf ($P < 0.01$ in bold).

Gene	2 dpf			8 dpf			20 dpf		
	MNC	LFC	*P*	MNC	LFC	*P*	MNC	LFC	*P*
dync2li1	96.09	−0.70	3.7E−05	34.05	−1.05	5.2E−05	23.83	−1.10	1.2E−01
pycr3	221.91	0.49	2.5E−03	56.19	1.09	1.5E−08	38.16	0.13	8.9E−01
eef1d	1984.23	0.18	1.3E−01	1076.82	0.51	8.8E−07	1265.39	0.08	8.9E−01
washc5	293.53	−0.14	5.0E−01	141.55	−0.40	9.2E−04	143.95	−0.03	9.6E−01
pxk	205.36	0.19	2.9E−01	183.15	0.67	1.9E−04	120.35	0.65	7.3E−02
hint1	1719.70	0.28	2.6E−01	824.17	0.46	9.4E−03	336.79	−1.03	9.7E−03
nsmce2	260.89	−0.48	1.4E−04	79.51	−0.44	1.5E−02	82.97	−0.80	6.1E−02
gimap2	17.46	2.14	5.5E−04	46.44	0.04	9.5E−01	57.94	1.89	1.6E−02
cdk5r1	106.52	−0.59	3.7E−03	292.02	0.31	9.2E−02	7.22	−1.18	3.6E−01
dph5	344.39	0.51	2.8E−03	108.03	0.20	2.9E−01	63.25	−0.28	6.4E−01
pdhb	662.23	0.41	6.9E−03	2359.84	0.06	8.1E−01	680.86	−0.29	5.8E−01
irf1	5.62	0.32	7.6E−01	142.62	−1.19	2.9E−04	360.24	1.17	1.0E−01

NOTE.—LFC, log2 fold change in expression (positive values indicate higher expression in scale-eaters than molluscivores); MNC, mean normalized counts across all samples; *P*, adjusted *P* value for differential expression (DESeq2).

reduced power to detect expression differences due to the small scale-eater sample size. Nonetheless, we found four genes differentially expressed throughout development at all three stages (*filip1*, *c1galt1*, *klhl24*, and *oit3*) and 248 genes were differentially expressed during two of the three stages examined. Of the 59 genes within 10 kb of SNPs or deletions fixed between species, we found 12 differentially expressed during at least one developmental stage (table 1 and fig. 4*E*). Two of these genes (*dync2li1* and *pycr3*) were differentially expressed at 2 and 8 dpf.

Since this is a young radiation, many other candidate adaptive loci are likely segregating between species due to incomplete hard sweeps or because multiple adaptive haplotypes exist causing signatures of soft sweeps. We also evaluated whether highly differentiated variants that were not fixed between species may influence expression divergence. Of the 1,940 genes within 20 kb of highly differentiated SNPs ($Fst > 0.72$ and $Dxy > 0.0083$), 384 were differentially expressed during at least one developmental stage (supplementary fig. S1, Supplementary Material online). This gene set was enriched for 87 biological processes, including pigment accumulation, vasculature development, lipid localization, and regulation of keratinocyte differentiation ($P < 0.05$; supplementary tables S4 and S5, Supplementary Material online).

Regulatory Mechanisms Underlying Expression Divergence between Species

Despite overall low genetic differentiation observed between species (genome-wide mean $Fst = 0.076$), we identified thousands of genes expressed in F1 hybrids containing heterozygous sites that were alternately homozygous between parental populations (ranging between 18.5% and 28.5% of all genes expressed in F1 hybrids; supplementary table S6, Supplementary Material online). We measured ASE for these genes using MBASED (Mayba et al. 2014) and inferred mechanisms of regulatory divergence by comparing the ratio of maternal and paternal allelic expression in F1 hybrids with the ratio of molluscivore and scale-eater gene expression in purebred F1 offspring (fig. 5; Cowles et al. 2002; Wittkopp et al. 2004; McManus et al. 2010; Mack et al. 2016).

Most genes were expressed at a similar level in each species, as well as in F1 hybrids, indicating conserved regulation (88.46–93.33%; fig. 6). The majority of genes that were differentially expressed between species showed *trans*-regulatory divergence (3.90–6.21%), which accounted for more than three times the number of genes influenced by *cis*-regulatory divergence (1.08–1.67%). *Trans*-regulatory divergence was also more prevalent than expression influenced by a combination of *cis* and *trans* effects. The number of genes influenced by *cis* × *trans* compensatory changes (0.80–2.25%) was similar to the number of genes influenced by *cis* + *trans* reinforcing changes (0.76–2.01%).

Cis-regulatory variants are expected to contribute to additive inheritance of gene expression in F1 hybrids, whereas *trans*-regulatory variants are expected to influence patterns of dominance (Prud'homme et al. 2007; Lemos et al. 2008; Signor and Nuzhdin 2018). Furthermore, *cis* × *trans* compensatory changes can result in transgressive gene expression, where expression is significantly higher or lower in F1 hybrids compared with parental populations (Landry et al. 2005, 2007; Mack et al. 2016; McGirr and Martin 2019). We found additive, dominant, and transgressive patterns of gene expression inheritance in F1 hybrids at both developmental stages. Despite the overall lower contribution of *cis*-regulatory divergence compared with *trans*-regulatory divergence, we found that slightly more genes showed additive inheritance than dominant inheritance (supplementary fig. S2, Supplementary Material online; 2 dpf: additive = 4.49% dominant = 1.90%; 8 dpf: additive = 5.84% dominant = 3.85%).

Fixed Variants near Genes Showing Cis-Regulatory Divergence

Although most differential expression between species was explained by *trans*-regulatory divergence, it is difficult to identify the downstream targets of *trans*-acting alleles because they are necessarily unlinked from the genes they regulate. Furthermore, it is unknown whether the predominance of

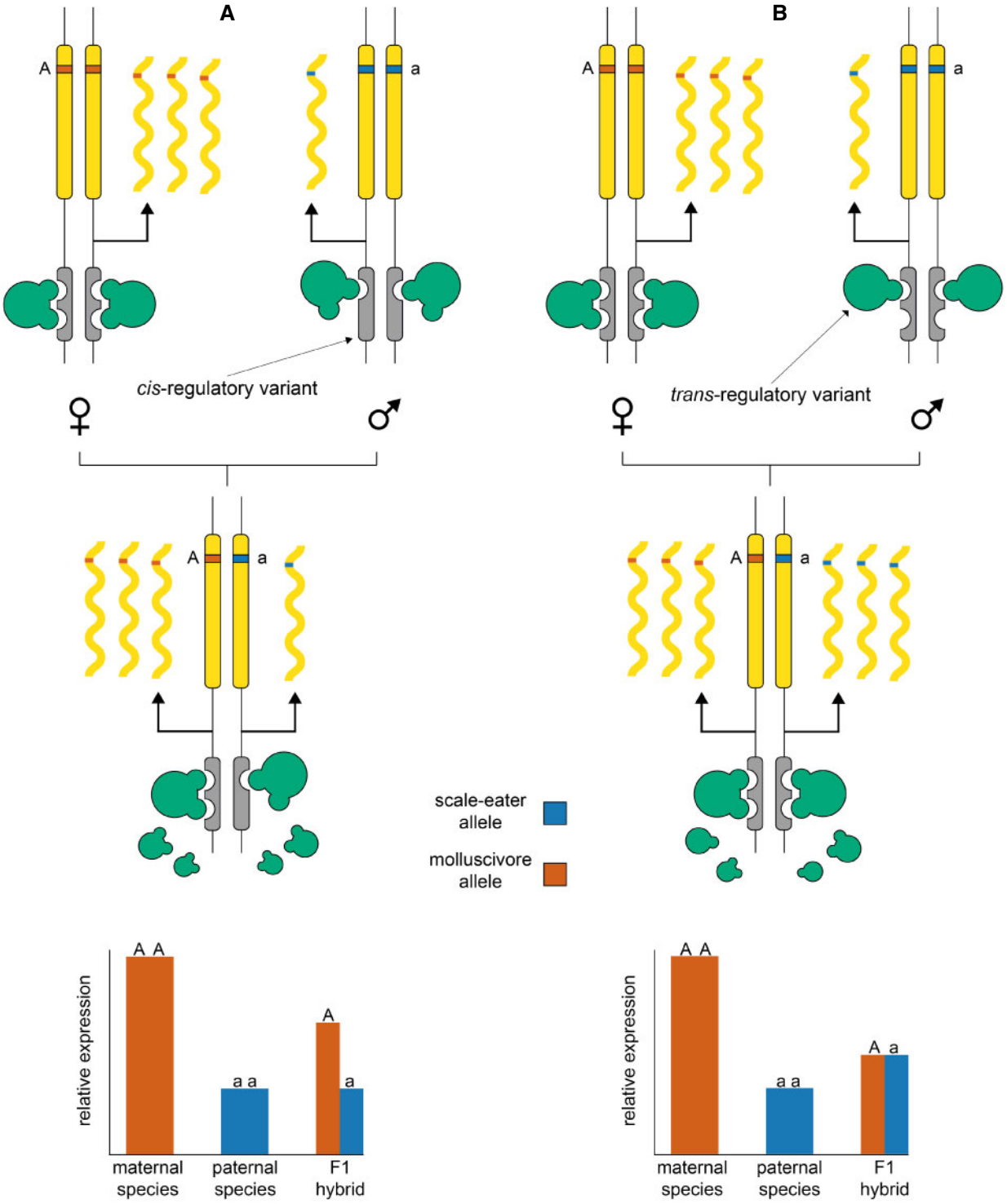

Fig. 5. Deciphering between *cis*- and *trans*-regulatory divergence influencing gene expression. Diagrams show protein coding gene regions (yellow) regulated by linked *cis*-acting elements (gray) and *trans*-acting-binding proteins (green). In the examples, a female molluscivore is crossed with a male scale-eater to produce an F1 hybrid. The two species are alternatively homozygous for an allele within the coding region of a gene that shows higher expression in the molluscivore than the scale-eater. (*A*) A *cis*-acting variant causing reduced expression results in low expression of the scale-eater allele in the F1 hybrid. (*B*) Lower expression in the scale-eater is caused by a *trans*-acting variant, resulting in similar expression levels of both parental alleles in the F1 hybrid.

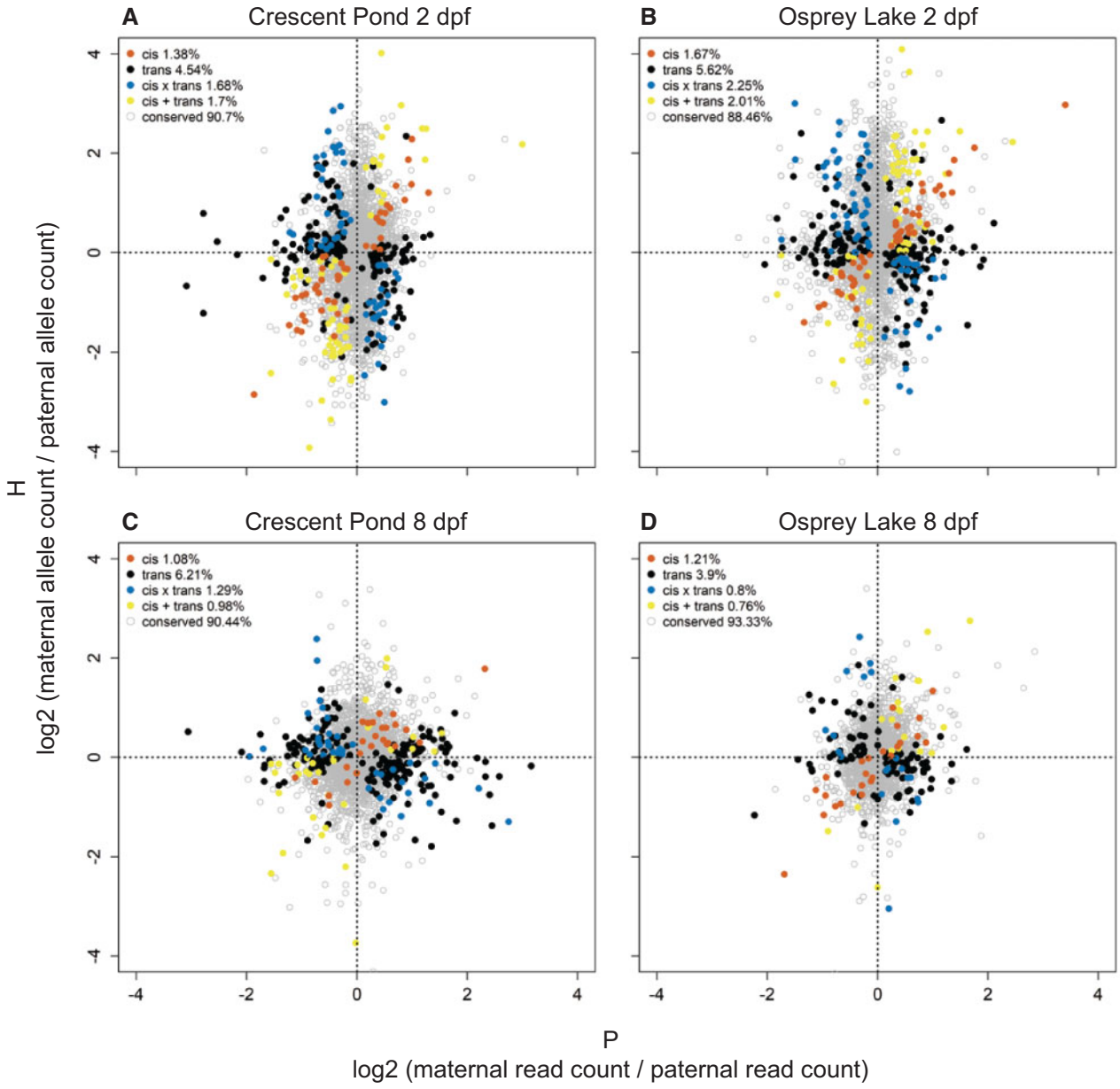

Fig. 6. Regulatory mechanisms underlying expression divergence between species. The ratio of maternal and paternal allelic expression in F1 hybrids (H) relative to the ratio of molluscivore and scale-eater gene expression in purebred F1 offspring (P) for genes containing heterozygous sites. Left panels show expression in Crescent Pond samples and right panels show Osprey Lake samples. Red = *cis* (significant ASE in F1 hybrids, significant differential expression between species, and no significant *trans*- contribution), black = *trans* (significant ASE in hybrids, significant differential expression between species, and significant *trans*-contribution), blue = *cis* × *trans* (*cis* and *trans* effects show opposing signs, significant ASE, no significant differential expression between species, significant *trans*-contribution), yellow = *cis* + *trans* (*cis* and *trans* effects show the same sign, significant ASE, no significant differential expression between species, significant *trans*-contribution), gray = conserved (no differential expression between species and no ASE).

trans-regulatory divergence was driven by few alleles with numerous effects or many alleles distributed throughout the genome. Thus, to identify candidate variation causing differences in gene expression between molluscivores and scale-eaters, we examined genes in highly differentiated regions of the genome that were differentially expressed due to *cis*-regulatory divergence. We found a total of 148 genes showing *cis*-regulatory divergence among all four F1 hybrid crosses (fig. 6). We identified 37 of these genes (25%) within the set of 384 genes that were differentially expressed between species and within 20 kb of highly differentiated SNPs ($Fst > 0.72$ and $Dxy > 0.0083$; supplementary table S7, Supplementary Material online).

We also found differentially expressed genes showing *cis*-regulatory divergence that were near the most highly differentiated regions of the genome containing variants fixed between species. Of the 12 genes that were within 10 kb of fixed variants, five contained heterozygous sites that could be used to measure ASE (fig. 7 and supplementary fig. S3, Supplementary Material online). Three of these (*eef1d*,

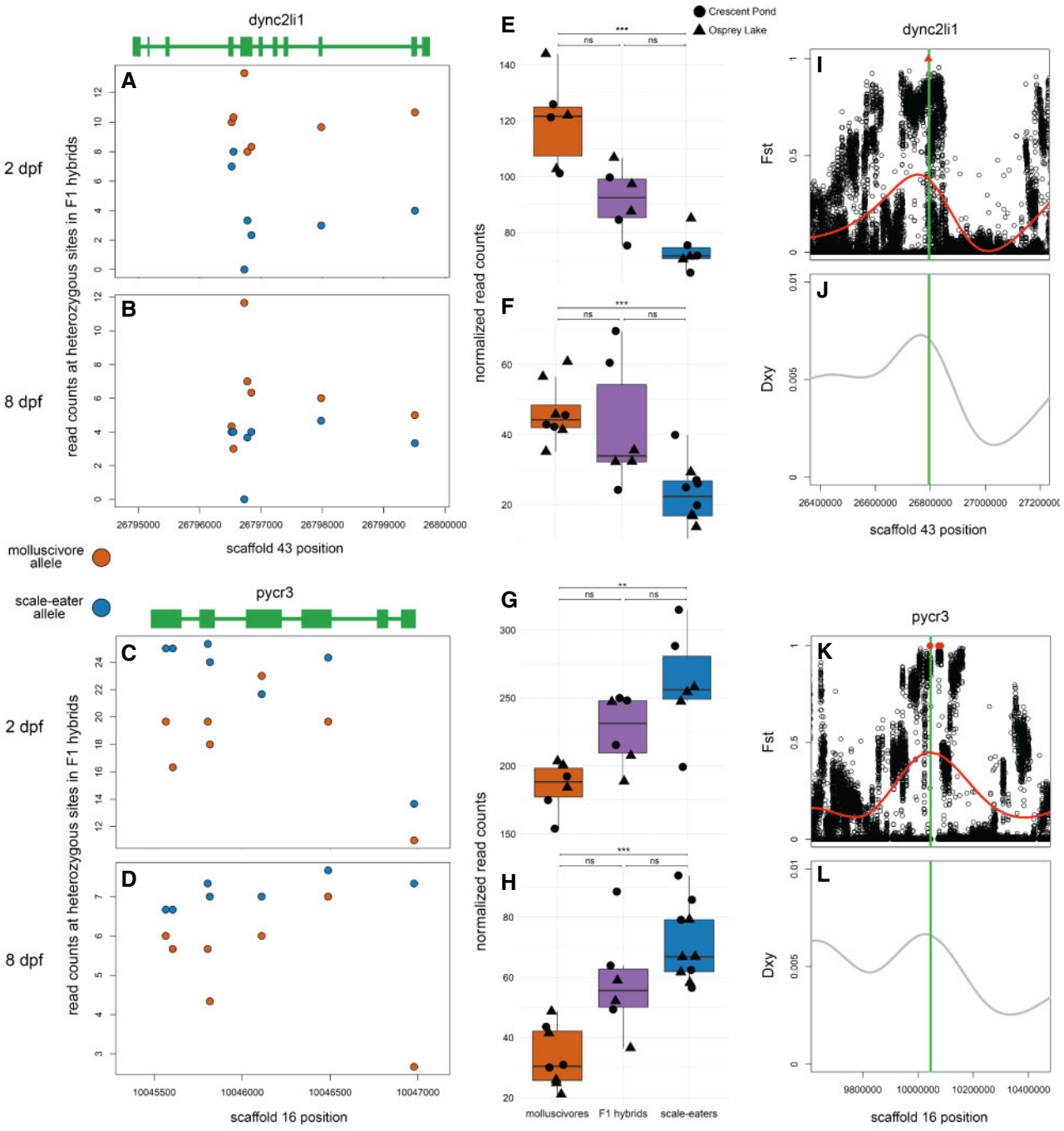

FIG. 7. Two genes near fixed variants show *cis*-regulatory divergence between trophic specialists. (*A*–*D*) Mean counts for reads spanning *dync2li1* and *pycr3* that match parental alleles at heterozygous sites are shown for crosses between Crescent Pond molluscivores (red) and scale-eaters (blue) at 2 dpf (*A* and *C*) and 8 dpf (*B* and *D*). (*E*–*H*) Normalized read counts for F1 offspring from Crescent Pond (circles) and Osprey Lake (triangles) crosses. Both genes are differentially expressed between molluscivores (red) and scale-eaters (blue) at both developmental stages and show additive inheritance in F1 hybrids (gray; $P < 0.01$*, 0.001**, 0.0001***, $P > 0.01$ ns). For both genes, F1 hybrids show higher expression of alleles derived from the parental species that shows higher gene expression in purebred F1 offspring (MBASED $P < 0.05$) and show *cis*-regulatory divergence between species. (*I*–*L*) Both genes (green lines) are within regions showing high relative genetic differentiation (*Fst*; *I* and *K*) and high absolute genetic divergence (*Dxy*; *J* and *L*). Red triangle shows fixed deletion. Red points show fixed SNPs (*Fst* = 1).

washc5, and *pxk*) showed *trans*-regulatory divergence (supplementary fig. S3, Supplementary Material online). The other two genes which were differentially expressed at 2 and 8 dpf (*dync2li1* and *pycr3*) showed *cis*-regulatory divergence (fig. 7). This provided strong evidence that differential regulation of these genes was influenced by genetic divergence within putative *cis*-regulatory elements.

These two genes showing *cis*-regulatory divergence were near just one fixed variant each: a 91 bp deletion located 7,384 bp upstream of *dync2li1* and an A-to-C transversion

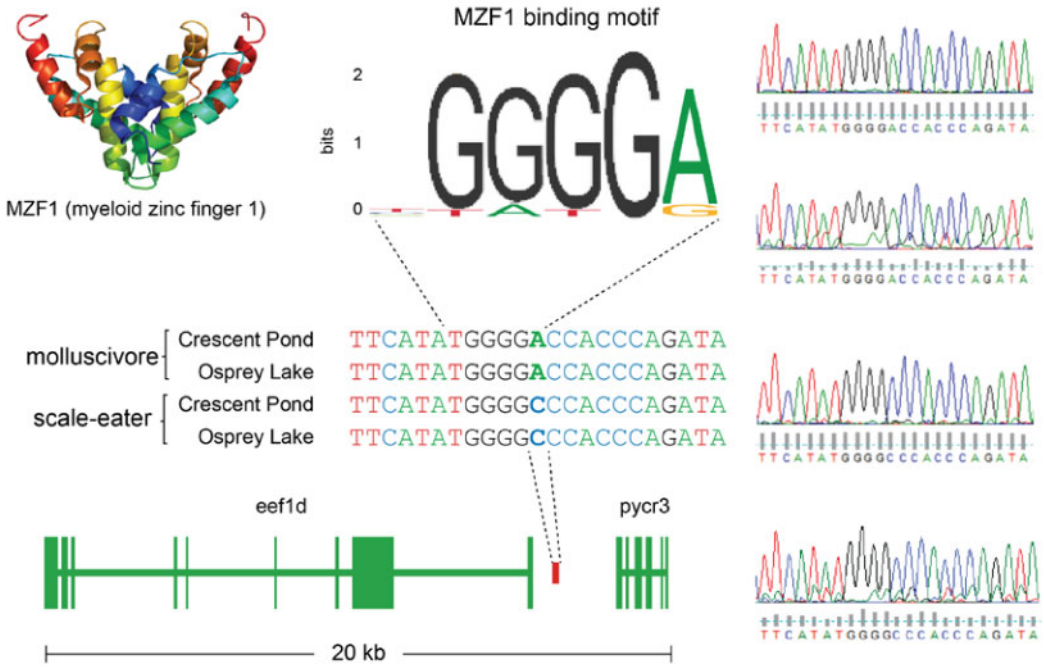

Fig. 8. Sanger sequencing confirms fixed SNP that could alter transcription factor binding near *pycr3*. Chromatograms on the right confirm the A-to-C transversion fixed in scale-eaters that falls between *eef1d* (supplementary fig. S3, Supplementary Material online) and *pycr3* (fig. 7). The myeloid zinc finger transcription factor binds a motif that matches the molluscivore (JASPAR database matrix ID: MA0056.1), however, the scale-eater allele alters this motif.

1,808 bp downstream of *pycr3* (fig. 7). The next closest fixed variants were separated by greater than 600 kb and 31 kb, respectively. We searched the JASPAR database (Fornes et al. 2019) to identify potential transcription factor-binding sites that could be altered by these candidate *cis*-acting variants. The 91 bp deletion near *dync2li1* contained binding motifs corresponding to seven transcription factors (*nfia*, *nfix*, *nfic*, *znf384*, *hoxa5*, *gata1*, *myb*; supplementary table S8, Supplementary Material online). Two binding motifs spanned the *pycr3* SNP region (*gata2*, *mzf1*), one of which, *mfz1*, was altered by the alternate allele in scale-eaters. The scale-eater allele created a new potential-binding motif matching the transcription factor *plagl2*. Sanger sequencing confirmed the A-to-C transversion near *pycr3* in four additional individuals not included in the whole-genome resequencing data set (fig. 8).

Discussion

Understanding the developmental genetic basis of complex traits by investigating natural variation among closely related species is a powerful complementary approach to traditional genetic screens in model systems. The San Salvador Island *Cyprinodon* pupfish system is a useful evolutionary model for understanding the genetic basis of craniofacial defects and natural diversity given extensive morphological divergence between these young species (fig. 1). We found thousands of genetic variants that were highly differentiated between molluscivore and scale-eater species that were near genes that were differentially expressed at multiple developmental stages. Just 244 variants were fixed between species across 9.3 million SNPs and 80,012 structural variants (fig. 2A and C). Almost all fixed variants were in noncoding regions, with the exception of an exon-spanning deletion (fig. 3). In support of these variants affecting divergent adaptive phenotypes, 80 variants were near 59 genes that were enriched for developmental functions related to divergent specialist traits (fig. 2B and D). Furthermore, 12 of these genes were highly differentially expressed between species across three developmental stages (fig. 4E). By measuring ASE in F1 hybrids from multiple crosses between species, we found that *trans*-regulatory divergence explained most patterns of expression divergence. We also identified two highly differentiated variants that may act as *cis*-regulatory alleles affecting expression divergence between species: a fixed deletion near *dync2li1* and a fixed SNP near *pycr*3 (fig. 7).

Gene Regulatory Divergence during Rapid Speciation

Other studies investigating *cis*- and *trans*-regulatory mechanisms have found that *cis*-acting alleles contribute more to interspecific divergence, whereas *trans*-acting alleles contribute more to intraspecific divergence (Prud'homme et al. 2007; Lemos et al. 2008; Signor and Nuzhdin 2018). Importantly, many of the studies supporting this pattern examine interspecific hybrids generated by species pairs with much greater divergence times (Graze et al. 2009: *Drosophila melanogaster* and *D. simulans* diverged 2.5 Ma; Tirosh et al. 2009: *Saccharomyces cerevisiae* and *S. paradoxus* diverged 5 Ma; Shi et al. 2012: *Arabidopsis thaliana* and *A. arenosa* diverged 5.3 Ma). Given that molluscivores and scale-eaters rapidly diverged within the past 10,000 years and are known to hybridize in the wild, we may see *trans*-effects dominating for

the same reasons *trans*-effects are thought to contribute more to intraspecific divergence. This is because, both within species and between young species pairs, the larger mutational target of *trans*-regulatory factors results in the observed excess of *trans*-effects (Wittkopp et al. 2008; Emerson et al. 2010; Suvorov et al. 2013).

Similar to other studies, we found predominately additive patterns of gene inheritance in F1 hybrids (Hughes et al. 2006; Rottscheidt and Harr 2007; Davidson and Balakrishnan 2016). However, this contrasts with our finding of wide-spread *trans*-regulatory divergence, which is expected to contribute to dominant and recessive patterns of inheritance (Lemos et al. 2008; Signor and Nuzhdin 2018). Since genes were required to contain heterozygous sites in F1 hybrids for ASE analyses, we were only able to classify mechanisms of regulatory divergence for a subset of genes used to classify modes of inheritance (supplementary table S6, Supplementary Material online). It is possible that heterozygous genes were biased to show *trans*-regulatory divergence. It is also possible that we underestimated the number of genes showing *cis*-regulatory divergence between species. We required that genes show ASE across the entire coding region to assign *cis*-regulatory divergence, which ignored the possibility of alleles affecting the expression of specific transcript isoforms.

Fixed Genetic Variation Influencing Trophic Specialization

In a previous analysis of SNPs from a smaller whole-genome data set, *dync2li1* was one of 30 candidate genes that showed signs of a hard selective sweep and was significantly associated with variation in jaw size between molluscivores and scale-eaters using multiple genome-wide association mapping approaches (McGirr and Martin 2017). Here, we show that a fixed deletion near *dync2li1* may influence expression divergence between species through *cis*-acting regulatory mechanisms. This gene (dynein cytoplasmic 2 light intermediate chain 1) is known to influence skeletal morphology in humans (Kessler et al. 2015; Taylor et al. 2015; Niceta et al. 2018). It is a component of the cytoplasmic dynein 2 complex which is important for intraflagellar transport—the movement of protein particles along the length of eukaryotic cilia (Cole 2003; Pfister et al. 2006). Due to the vital role that cilia play in the transduction of signals in the *hedgehog* pathway and other pathways important for skeletal development, disruptions in dynein complexes cause a variety of skeletal dysplasias collectively termed skeletal ciliopathies (Huber and Cormier-Daire 2012; Taylor et al. 2015). Mutations in *dync2li1* have been linked with ciliopathies that result from abnormal cilia shape and function including Ellis-van Creveld syndrome, Jeune syndrome, and short rib polydactyly syndrome (Kessler et al. 2015; Taylor et al. 2015; Niceta et al. 2018). These disorders are characterized by variable craniofacial malformations including micrognathia (small jaw), hypodontia (tooth absence), and cleft palate (Brueton et al. 1990; Ruiz-Perez and Goodship 2009; Taylor et al. 2015). The discovery of *dync2li1* as a candidate gene influencing differences in oral jaw length between molluscivores and scale-eaters suggests that this system is particularly well-suited as an evolutionary mutant model for clinical phenotypes involving jaw size, such as micrognathia and macrognathia.

We also identified a fixed SNP near the gene *pycr3* (pyrroline-5-carboxylate reductase 3; also denoted *pycrl*) which showed *cis*-regulatory divergence. This gene is not currently known to influence craniofacial phenotypes in humans or other model systems. However, one study investigating gene expression divergence between beef and dairy breed bulls found that *pycr3* was one of the most highly differentially expressed genes in skeletal muscle tissues. The authors found nearly a 3-fold difference in expression of *pycr3* between the two bull breeds that are primarily characterized by differences in muscle anatomy (Sadkowski et al. 2009). Similarly, expression changes in this gene may influence skeletal muscle development in specialists species, which differ in the size of their adductor mandibulae muscles (Martin and Wainwright 2011; Hernandez et al. 2018). The A-to-C transversion near *pycr3* could influence differences in expression by altering transcription factor binding. We found that the molluscivore allele matches the binding motif of *mzf1* (myeloid zinc finger 1; fig. 8), a transcription factor known to influence cell proliferation (Gaboli et al. 2001), whereas the scale-eater allele alters this motif. This type of binding motif analysis has a high sensitivity (*mzf1* is known to bind this motif) but extremely low selectivity (*mzf1* does not bind nearly every occurrence of this motif, which appears 1,430,540 times in the molluscivore reference genome).

Although oral jaw size is the primary axis of phenotypic divergence in the San Salvador Island pupfish system, adaptation to divergent niches required changes in a suite of morphological and behavioral phenotypes (St. John et al. 2019; St. John et al. 2020b). Most genes differentially expressed between species were found within whole embryo tissues (fig. 4A–D), suggesting we should find candidate genes influencing the development of craniofacial phenotypes and other divergent traits. Of the 244 variants fixed between species, the only coding variant was a 1,256 bp deletion that spanned the fifth exon of *gpa33* (glycoprotein A33), which is expressed exclusively in intestinal epithelium (fig. 3). Knockouts of this gene in mice cause increased hypersensitivity to food allergens and susceptibility to a range of related inflammatory intestinal pathologies (Williams et al. 2015). The gut contents of wild-caught scale-eaters comprised 40–51% scales (Martin and Wainwright 2013c). The exon deletion of *gpa33* may play a metabolic role in this unique adaptation that allows scale-eaters to occupy a higher trophic level than molluscivores. Future studies in this system will benefit from sequencing and analyses that target-specific tissues and cell types to determine whether candidate variants affect a single phenotype or have pleiotropic effects.

The Effectiveness of *Cyprinodon* Pupfishes for Identifying Candidate Cis-Regulatory Variants

One major advantage of investigating the genetic basis of craniofacial divergence between molluscivores and scale-eaters is the low amount of genetic divergence between species. Species-specific phenotypes are replicated across multiple isolated lake populations that exhibit substantial ongoing

gene flow. This has resulted in small regions of the genome showing strong genetic differentiation (63,542 SNPs showing $Fst > 0.72$ and $Dxy > 0.0083$), with some regions containing just a single variant fixed between species. The low number of fixed variants dispersed across the genome makes this system relatively unique compared with other systems with similar divergence times (Bernatchez et al. 2010; Jones et al. 2012; Martin et al. 2019).

A previous study found a significant QTL explaining 15% of variation in oral jaw size and three more potential moderate-effect QTL, suggesting that we may expect to find variants with moderate effects on craniofacial divergence. Variants with larger effect sizes are predicted to fix faster than variants with smaller effects, especially given short divergence times (Griswold 2006; Yeaman and Whitlock 2011; Stetter et al. 2018), which may suggest that the fixed variants near *dync2li1* and *pycr3* have larger effects than segregating candidate alleles. However, these fixed alleles are tightly linked with other highly differentiated alleles and may affect phenotypic divergence through combined small effects with many closely clustered variants. Furthermore, the fixation rate of mutations is not only dependent on effect size, but also dominance, which is an important mode of gene expression inheritance in this system (supplementary fig. S2, Supplementary Material online) and other systems (Gibson et al. 2004; Lemos et al. 2008; Signor and Nuzhdin 2018). While the fixed variants near *dync2li1* and *pycr3* represent promising candidate alleles, adaptive differences in craniofacial morphology are likely influenced by many loci, similar to polygenic traits studied in other systems (Bergland et al. 2014; Boyle et al. 2017; Barghi et al. 2019; Sella et al. 2019).

Conclusions

Overall, our results highlight the utility of the San Salvador Island pupfish system as an evolutionary mutant model for natural and clinical variation in human craniofacial phenotypes. Similar rapid speciation replicated across many environments can be found in other adaptive radiations (Martin et al. 2019; Martin and Richards 2019; Levin et al. 2020), which could also prove useful as evolutionary models for a variety of other human traits. We found that a combination of structural variant likely contributes to the evolution of highly divergent craniofacial morphology, and that *trans*-regulatory mechanisms dominate patterns of expression divergence between these young species. Future studies will attempt to validate the effect of candidate variation on gene expression and craniofacial development *in vivo*.

Materials and Methods

Identifying Genomic Variation Fixed between Specialists

To identify SNPs fixed between molluscivores and scale-eaters, we analyzed whole-genome resequencing samples for 258 individuals from across the Caribbean (median coverage = 8×; Richards et al. 2020). Briefly, 114 pupfishes from 15 isolated hypersaline lakes and one estuary on San Salvador Island were collected using hand and seine nets between 2011 and 2018. This included 33 generalists, 46 molluscivores, and 35 scale-eaters. Eight of these individuals were bred to generate F1 offspring sampled for RNA sequencing (supplementary table S3, Supplementary Material online). This data set also included 140 outgroup generalist pupfishes from across the Caribbean and North America, including two individuals belonging to the pupfish radiation in Lake Chichancanab, Mexico, and two individuals from the most closely related outgroups to *Cyprinodon* (*Megupsilon aporus* and *Cualac tessellatus*; Echelle et al. 2005). Libraries for 150PE Illumina sequencing were generated from DNA extracted from muscle tissue and the resulting reads were mapped to the *C. brontotheroides* reference genome (v 1.0; total sequence length = 1,162,855,435 bp; number of scaffolds = 15,698, scaffold N50, = 32,000,000 bp; L50 = 15 scaffolds; Richards et al. 2020). Variants were called using the HaplotypeCaller function of the Genome Analysis Toolkit (GATK v 3.5; DePristo et al. 2011). The GATK best practices workflow suggests using high-quality known variants to act as a reference to recalibrate variant quality scores. Due to the lack of a high confidence variant call set for this system, SNPs were filtered using conservative hard-filtering parameters (DePristo et al. 2011; Richards and Martin 2020). SNPs were further filtered to include SNPs with a minor allele frequency above 0.05, genotype quality above 20, and sites with greater than 50% genotyping rate across all individuals, resulting in 9.3 million SNPs.

Measuring relative genetic differentiation (*Fst*) between species can point to regions of the genome containing variation affecting divergent phenotypes (Jones et al. 2012; Poelstra et al. 2014; Lamichhaney et al. 2015). However, *Fst* is dependent on the many potential forces acting to reduce within-population nucleotide diversity, including selective sweeps, purifying selection, background selection, and low recombination rates (Noor and Bennett 2009; Cruickshank and Hahn 2014). Measuring between-population divergence (*Dxy*) can help distinguish between these possibilities because nucleotide divergence between species increases at loci under different selective regimes (Nachman and Payseur 2012; Cruickshank and Hahn 2014; Irwin et al. 2016). We measured *Fst* between species with vcftools (v. 0.1.15; weir-fst-pop function) and identified fixed SNPs ($Fst = 1$). We also measured *Fst* and *Dxy* in 10 and 20 kb windows using the python script popGenWindows.py created by Simon Martin (github.com/simonhmartin/genomics_general; Martin et al. 2013).

We identified structural variation (insertions, deletions, inversions, translocations, and copy number variants) fixed between specialist species with DELLY (v 0.8.1; Rausch et al. 2012). Unlike GATK HaplotypeCaller which is limited to identifying structural variants smaller than half the length of read size (DePristo et al. 2011), DELLY can identify small variants in addition to variants larger than 300 bp using paired-end clustering and split read analysis. We used DELLY to identify structural variants across eight whole genomes from the breeding pairs used to generate F1 hybrid RNA samples (four scale-eaters from two lake populations and four molluscivores from the same two lake populations; supplementary table S3, Supplementary Material online). First, we

trimmed reads using Trim Galore (v. 4.4, Babraham Bioinformatics), aligned them to the *C. brontotheroides* reference genome with the Burrows–Wheeler Alignment Tool (v 0.7.12; Li and Durbin 2011), and removed duplicate reads from the resulting .bam files with Picard MarkDuplicates (broadinstitute.github.io/picard). Second, we called variants with DELLY by comparing an individual of one species with all individuals of the other species, resulting in eight variant call files. Third, we identified structural variants fixed between species that were shared across all eight files, in which all molluscivores showed the reference allele and all scale-eaters showed the same alternate allele.

Transcriptomic Sequencing, Alignment, and Variant Discovery

Our transcriptomic data set included 50 libraries from 122 individuals sampled across three early developmental stages (supplementary table S3, Supplementary Material online; McGirr and Martin 2018, 2019). Breeding pairs used to generate F1 hybrids and purebred F1 offspring were collected from three hypersaline lakes on San Salvador Island: Crescent Pond, Osprey Lake, and Little Lake. For purebred crosses, we collected F1 embryos from breeding tanks containing multiple breeding pairs from a single lake population. For F1 hybrid samples, we crossed a single individual of one species with a single individual of another species from the same lake population.

RNA was extracted from samples collected 2 days after fertilization (2 dpf) 8 days after fertilization (8 dpf), and 17–20 days after fertilization (20 dpf) using RNeasy Mini Kits (Qiagen catalog no. 74104). For samples collected at 2 dpf, we pooled 5 embryos together and pulverized them in a 1.5 ml Eppendorf tube using a plastic pestle washed with RNase Away (Molecular BioProducts). We used the same extraction method for samples collected at 8 dpf but did not pool larvae and prepared a library for each individual separately. We dissected samples collected at 20 dpf to isolate tissues from the anterior craniofacial region containing the dentary, angular articular, maxilla, premaxilla, palatine, and associated craniofacial connective tissues using fine-tipped tweezers washed with RNase AWAY. All samples were reared in breeding tanks at 25–27 °C, 10–15 ppt salinity, pH 8.3, and fed a mix of commercial pellet foods and frozen foods.

Methods for total mRNA sequencing were previously described (McGirr and Martin 2018, 2019). Briefly, 2 and 8 dpf libraries were prepared using TruSeq stranded mRNA kits and sequenced on 3 lanes of Illumina 150 PE Hiseq4000 at the Vincent J. Coates Genomic Sequencing Center (McGirr and Martin 2019). All 20 dpf libraries were prepared using the KAPA stranded mRNA-seq kit at the High Throughput Genomic Sequencing Facility at UNC Chapel Hill and sequenced on one lane of Illumina 150PE Hiseq4000 (McGirr and Martin 2018). We filtered raw reads using Trim Galore (v. 4.4, Babraham Bioinformatics) to remove Illumina adaptors and low-quality reads (mean Phred score < 20) and mapped 122,090,823 filtered reads to the *C. brontotheroides* reference genome (Richards et al. 2020) using the RNAseq aligner STAR with default parameters (v. 2.5; Dobin et al. 2013). We assessed mapping and read quality using MultiQC (Ewels et al. 2016) and quantified the number of duplicate reads and the median percent GC content of mapped reads for each sample using RSeQC (Wang et al. 2012). Although all reads were mapped to a molluscivore reference genome, we did not find a significant difference between species in the proportion of reads uniquely mapped with STAR (supplementary fig. S4*A*, Supplementary Material online; Student's *t*-test, $P = 0.061$). In addition, we did not find a difference between species in the proportion of multimapped reads, GC content of reads, or number of duplicate reads (supplementary fig. S4*B–D*, Supplementary Material online; Student's *t*-test, $P > 0.05$).

We used GATK HaplotypeCaller function to call SNPs across 50 quality filtered transcriptomes. We refined SNPs using the allele-specific software WASP (v. 0.3.3) to correct for potential mapping biases that would influence tests of ASE (Van De Geijn et al. 2015). WASP identified reads that overlapped SNPs in the initial .bam files and remapped those reads after swapping the genotype for the alternate allele. Reads that failed to map to exactly the same location were discarded. We remapped unbiased reads to create our final .bam files used for differential expression analyses. Finally, we recalled SNPs using unbiased .bam files for ASE analyses.

Differential Expression Analyses

We used the featureCounts function of the Rsubread package (Liao et al. 2014) requiring paired-end and reverse stranded options to generate read counts across 19,304 genes and 156,743 exons annotated for the molluscivore (*C. brontotheroides*) reference genome (Richards et al. 2020). We used DESeq2 (v. 3.5; Love et al. 2014) to normalize raw read counts for library size and perform principal component analyses, and identify differentially expressed genes. DESeq2 fits negative binomial generalized linear models for each gene across samples to test the null hypothesis that the fold change in gene expression between two groups is zero. Significant differential expression between groups was determined with Wald tests by comparing normalized posterior log fold change estimates and correcting for multiple testing using the Benjamini–Hochberg procedure with a false discovery rate of 0.01 (Benjamini and Hochberg 1995).

We constructed a DESeqDataSet object in R using a multifactor design that accounted for variance in F1 read counts influenced by parental population origin and sequencing date (design = ~sequencing_date + parental_breeding_pair_populations). Next, we used a variance stabilizing transformation on normalized counts and performed a principal component analysis to visualize the major axes of variation in 2, 8, and 20 dpf samples (supplementary fig. S5, Supplementary Material online). We contrasted gene expression in pairwise comparisons between species grouped by developmental stage (sample sizes for comparisons [molluscivores vs. scale-eaters]: 2 dpf = 6 vs. 6, 8 dpf = 8 vs. 10, 20 dpf = 6 vs. 2).

We used plyranges (v. 1.6.5; Lee et al. 2019) to identify genetic variants overlapping with gene regions. For each gene we identified variants within 10 kb of the start of the

first exon and within 10 kb of the end of the last exon. We also searched within 20 kb of genes, which is the distance at which linkage disequilibrium decays to background levels (McGirr and Martin 2017). Using these window sizes, we were only able to identify differentiated regions of the genome as candidate *cis*-regulatory regions that may influence expression levels of linked genes. This approach does not take into account the action of distal regulatory regions acting at longer ranges.

Allele-Specific Expression Analyses

Our SNP data set included every parent used to generate F1 hybrids between populations ($n = 8$). We used the GATK VariantsToTable function (DePristo et al. 2011) to output genotypes across 9.3 million SNPs for each parent and overlapped these sites with the variant sites identified in F1 hybrid transcriptomes. We used python scripts (github.com/joemcgirr/fishfASE) to identify SNPs that were alternatively homozygous in breeding pairs and heterozygous in their F1 offspring. We counted reads across heterozygous sites using ASEReadCounter (–minDepth 20 –minMappingQuality 10 –minBaseQuality 20 –drf DuplicateRead) and matched read counts to maternal and paternal alleles.

We identified significant ASE using a beta-binomial test comparing the maternal and paternal counts at each gene with the R package MBASED (Mayba et al. 2014). For each F1 hybrid sample, we performed a 1-sample analysis with MBASED using default parameters run for 1,000,000 simulations to determine whether genes showed significant ASE in hybrids ($P < 0.05$). To test whether certain types of genes were disproportionally included or excluded from ASE analyses due to the requirement that a gene contain heterozygous sites in F1 hybrids, we determined how many of these genes were annotated for effects on cranial skeletal system development (GO:1904888) and skeletal system development (GO:0048705). We performed Fisher's exact tests for each cross, testing the null hypothesis that the proportion of heterozygous genes within an ontology was equal to the proportion of noninformative genes within an ontology. We did not find that genes involved in skeletal development were disproportionally excluded from ASE analyses due to the requirement that a gene contain heterozygous sites (Fisher's exact test, $P > 0.05$; supplementary table S9, Supplementary Material online).

Classifying Regulatory Mechanisms and Inheritance in F1 Hybrids

It is possible to identify mechanisms of gene expression divergence between parental species by bringing *cis* elements from both parents together in the same *trans* environment in F1 hybrids and quantifying ASE of parental alleles at heterozygous sites (fig. 5; Cowles et al. 2002; Wittkopp et al. 2004). A gene that is differentially expressed between parental species that also shows ASE biased toward one parental allele is expected to result from *cis*-regulatory divergence. A gene that is differentially expressed between parental species that does not show ASE in F1 hybrids is expected to result from *trans*-regulatory divergence.

To determine regulatory mechanisms controlling expression divergence between parental species, a gene had to be included in differential expression analyses and ASE analyses. We required that genes had at least two informative SNPs with $\geq 10\times$ coverage to assign regulatory mechanisms. We calculated H—the ratio of maternal allele counts compared with the number of paternal allele counts in F1 hybrids, and P—the ratio of normalized read counts in purebred F1 offspring from the maternal population compared with read counts in purebred F1 offspring from the paternal population. We performed a Fisher's exact test using H and P to determine whether there was a significant *trans*- contribution to expression divergence (T), testing the null hypothesis that the ratio of read counts in the parental populations was equal to the ratio of parental allele counts in hybrids (Wittkopp et al. 2004; McManus et al. 2010; Goncalves et al. 2012; Mack et al. 2016).

For each lake population at each developmental stage, we classified expression divergence due to *cis*-regulation if a gene showed significant ASE in all F1 hybrids, significant differential expression between parental populations of purebred F1 offspring, and no significant T. We identified expression divergence due to *trans*-regulation if genes did not show ASE, were differentially expressed between parental populations, and showed significant T. We defined *cis*- × *trans*-regulatory divergence if a gene showed H and P with opposing signs (*cis*- and *trans*-regulatory factors had opposing effects on expression), significant ASE, significant T, and was not differentially expressed between parental populations. We defined *cis*- + *trans*-regulatory divergence if a gene showed H and P with the same sign (*cis*- and *trans*-regulatory factors had the same effect on expression), significant ASE, significant T, and was not differentially expressed between parental populations (McManus et al. 2010; Coolon et al. 2014; Mack et al. 2016).

For each developmental stage, we grouped species and F1 hybrids by lake population and compared expression in F1 hybrids to expression in purebred offspring to determine whether genes showed additive, dominant, or transgressive patterns of inheritance in hybrids. We conducted four pairwise differential expression tests with DESeq2: 1) molluscivores versus scale-eaters, 2) molluscivores versus F1 hybrids, 3) scale-eaters versus F1 hybrids, 4) molluscivores and scale-eaters versus F1 hybrids. Hybrid inheritance was considered additive if hybrid gene expression was intermediate between parental populations and significantly different between parental populations. Inheritance was dominant if hybrid expression was significantly different from one parental population but not the other. Genes showing misexpression in hybrids showed transgressive inheritance, meaning hybrid gene expression was significantly higher (overdominant) or lower (underdominant) than both parental species.

Gene Ontology Enrichment and Transcription Factor-Binding Site Analyses

We performed gene ontology (GO) enrichment analyses for genes near candidate adaptive variants using ShinyGo v.0.51 (Ge et al. 2020). The *C. brontotheroides* reference genome was annotated using MAKER, a genome annotation pipeline that

annotates genes, transcripts, and proteins (Cantarel et al. 2007). Gene symbols for orthologs identified by this pipeline largely match human gene symbols. Thus, we searched for enrichment across biological process ontologies curated for human gene functions.

We searched the JASPAR database (Fornes et al. 2019) to identify whether fixed variation near genes showing *cis*-regulatory divergence altered potential transcription factor-binding sites. We generated fasta sequences for the molluscivore containing the variant site and 20 bp on either end of the site and searched across all 1,011 predicted vertebrate-binding motifs in the database using a 95% relative profile score threshold. We then preformed the same analysis for scale-eater fasta sequences containing the alternate allele.

Genotyping Fixed Variants

To confirm the genotypes of putative *cis*-acting variants, we performed Sanger sequencing on four additional individuals that were not included in our whole-genome data set. We extracted DNA from muscle tissue using DNeasy Blood and Tissue kits (Qiagen, Inc.) from two molluscivores and two scale-eaters (wild samples were collected from Crescent Pond and Osprey Lake for both species). We designed primers targeting the regions containing variation fixed between species near the two genes showing evidence for *cis*-regulatory divergence (*pycr3* and *dync2li1*) using the NCBI primer design tool (Ye et al. 2012). We designed primers targeting a 446 bp region containing the SNP fixed between species (scaffold: HiC_scaffold_16; position: 10,043,644) that was 1,808 bp downstream of *pycr3* (forward: 5′-ACCATTCCAGAAGACAAAAAGCG-3′; reverse: 5′-GGCCCTATATATGGGATGCACAA-3′). Sequences were amplified with PCR using New England BioLabs *Taq* polymerase (no. 0141705) and dNTP solution (no. 0861609) and Sanger sequencing was performed at Eton Bioscience, Inc. (Research Triangle Park, NC). Aligning the resulting sequences using the Clustal Omega Multiple Sequence Alignment Tool (Madeira et al. 2019) confirmed the A-to-C transversion in scale-eaters (fig. 8). We designed two additional primer sets targeting the deletion region near *dync2li1* (scaffold: HiC_scaffold_43; position: 26,792,380–26,792,471). Although both primer sets amplified the sequence in molluscivore samples (not shown), we were unable to amplify this region in scale-eaters, potentially due to high polymorphism in this region.

Supplementary Material

Supplementary data are available at *Molecular Biology and Evolution* online.

Acknowledgments

This study was funded by the University of North Carolina at Chapel Hill, the University of California, Berkeley, NSF CAREER Award 1749764, and NIH/NIDCR R01 DE027052 to C.H.M. and a Graduate Research Fellowship from the Triangle Center for Evolutionary Medicine and an SSE Rosemary Grant Travel Award to J.A.M. We thank Daniel Matute, Emilie Richards, Michelle St. John, Bryan Reatini, and Sara Suzuki for valuable discussion; The Vincent J. Coates Genomics Sequencing Laboratory at the University of California, Berkeley for performing RNA library prep and Illumina sequencing; the Gerace Research Centre for logistics; and the Bahamian government BEST Commission for permission to conduct this research.

Author Contributions

J.A.M. wrote the manuscript, extracted the RNA samples, and conducted all bioinformatic and population genetic analyses. Both authors contributed to the conception and development of the ideas and revision of the manuscript.

Data Accessibility

All transcriptomic raw sequence reads are available as zipped fastq files on the NCBI BioProject database. Accession: PRJNA391309. Title: Craniofacial divergence in Caribbean Pupfishes. All R and Python scripts used for pipelines are available on Github (github.com/joemcgirr/fishfASE).

References

Ahi EP, Kapralova KH, Pálsson A, Maier VH, Gudbrandsson J, Snorrason SS, Jónsson ZO, Franzdóttir SR. 2014. Transcriptional dynamics of a conserved gene expression network associated with craniofacial divergence in Arctic charr. *Evodevo*. 5(1):40.

Albertson RC, Cresko W, Iii HWD, Postlethwait JH. 2008. Evolutionary mutant models for human disease. *Trends Genet*. 25:74–81.

Albertson RC, Streelman JT, Kocher TD, Yelick PC. 2005. Integration and evolution of the cichlid mandible: the molecular basis of alternate feeding strategies. *Proc Natl Acad Sci*. 102(45):16287–16292.

Barghi N, Tobler R, Nolte V, Jakšić AM, Mallard F, Otte KA, Dolezal M, Taus T, Kofler R, Schlötterer C. 2019. Genetic redundancy fuels polygenic adaptation in *Drosophila*. *PLoS Biol*. 17:e3000128.

Benjamini Y, Hochberg. 1995. Controlling the falsediscovery rate: a practical and powerful approach to multiple testing. *J R Statsoc Series B*. 57(1):289.

Bergland AO, Behrman EL, O'Brien KR, Schmidt PS, Petrov DA. 2014. Genomic evidence of rapid and stable adaptive oscillations over seasonal time scales in *Drosophila*. *PLoS Genet*. 10(11):e1004775.

Bernatchez L, Renaut S, Whiteley AR, Derome N, Jeukens J, Landry L, Lu G, Nolte AW, Østbye K, Rogers SM, et al. 2010. On the origin of species: insights from the ecological genomics of lake whitefish. *Phil Trans R Soc B* 365(1547):1783–1800.

Bono JM, Olesnicky EC, Matzkin LM. 2015. Connecting genotypes, phenotypes and fitness: harnessing the power of CRISPR/Cas9 genome editing. *Mol Ecol*. 24(15):3810–3822.

Boyle EA, Li YI, Pritchard JK. 2017. An expanded view of complex traits: from polygenic to omnigenic. *Cell [Internet]* 169(7):1177–1186.

Brueton LA, Dillon MJ, Winter RM. 1990. Ellis-van Creveld syndrome, Jeune syndrome, and renal-hepatic-pancreatic dysplasia: separate entities or disease spectrum? *J Med Genet*. 27(4):252–255.

Cantarel BL, Korf I, Robb SMC, Parra G, Ross E, Moore B, Holt C, Alvarado AS, Yandell M. 2007. MAKER: an easy-to-use annotation pipeline designed for emerging model organism genomes. *Genome Res*. 18(1):188–196.

Cleves PA, Ellis NA, Jimenez MT, Nunez SM, Schluter D, Kingsley DM, Miller CT. 2014. Evolved tooth gain in sticklebacks is associated with a *cis*-regulatory allele of Bmp6. *Proc Natl Acad Sci*. 111(38):13912–13917. [Internet]

Cole DG. 2003. The intraflagellar transport machinery of *Chlamydomonas reinhardtii*. *Traffic* 4(7):435–442.

Conway JR, Lex A, Gehlenborg N. 2017. UpSetR: an R package for the visualization of intersecting sets and their properties. *Bioinformatics* 33(18):2938–2940.

Coolon JD, Mcmanus CJ, Stevenson KR, Coolon JD, Mcmanus CJ, Stevenson KR, Graveley BR, Wittkopp PJ. 2014. Tempo and mode of regulatory evolution in *Drosophila* Tempo and mode of regulatory evolution in *Drosophila*. *Genome Res*. 24(5):797–808.

Cowles CR, Hirschhorn JN, Altshuler D, Lander ES. 2002. Detection of regulatory variation in mouse genes. *Nat Genet*. 32(3):432–437.

Cruickshank TE, Hahn MW. 2014. Reanalysis suggests that genomic islands of speciation are due to reduced diversity, not reduced gene flow. *Mol Ecol*. 23(13):3133–3157.

Davidson JH, Balakrishnan CN. 2016. Gene regulatory evolution during speciation in a songbird. 6:1357–1364.

DePristo MA, Banks E, Poplin R, Garimella KV, Maguire JR, Hartl C, Philippakis AA, del Angel G, Rivas MA, Hanna M, et al. 2011. A framework for variation discovery and genotyping using next-generation DNA sequencing data. *Nat Genet*. 43(5):491–498.

Dobin A, Davis CA, Schlesinger F, Drenkow J, Zaleski C, Jha S, Batut P, Chaisson M, Gingeras TR. 2013. STAR: ultrafast universal RNA-seq aligner. *Bioinformatics* 29(1):15–21.

Echelle AA, Carson EW, Echelle AF, Van Den Bussche RA, Dowling TE, Meyer A. 2005. 2005. Historical biogeography of the new-world pupfish genus Cyprinodon (Teleostei: Cyprinodontidae). *Copeia* 2005(2):320–339.

Emerson JJ, Hsieh L-C, Sung H-M, Wang T-Y, Huang C-J, Lu H-S, Lu J, Wu S-H, Li W-H. 2010. Natural selection on cis and trans regulation in yeasts. *Genome Res*. 20(6):826–836.

Erickson PA, Baek J, Hart JC, Cleves PA, Miller CT. 2018. Genetic dissection of a supergene implicates tfap2a in craniofacial evolution of threespine sticklebacks. *Genetics* 209(2):591–605.

Ewels P, Magnusson M, Lundin S, Käller M. 2016. Data and text mining MultiQC: summarize analysis results for multiple tools and samples in a single report. *Bioinformatics* 32(19):3047–3048.

Fornes O, Castro-Mondragon JA, Khan A, van der Lee R, Zhang X, Richmond PA, Modi BP, Correard S, Gheorghe M, Baranašić D. 2019. JASPAR 2020: update of the open-access database of transcription factor binding profiles. *Nucleic Acids Res*. 48:87–92.

Furutani-Seiki M, Wittbrodt J. 2004. Medaka and zebrafish, an evolutionary twin study. *Mech Dev*. 121(7–8):629–637.

Gaboli M, Kotsi PA, Gurrieri C, Cattoretti G, Ronchetti S, Cordon-Cardo C, Broxmeyer HE, Hromas R, Pandolfi PP. 2001. Mzf1 controls cell proliferation and tumorigenesis. *Genes Dev*. 15(13):1625–1630.

Ge SX, Jung D, Yao R. 2020. ShinyGO: a graphical gene-set enrichment tool for animals and plants. *Bioinformatics* 36(8):2628–2629.

Gibson G, Riley-Berger R, Harshman L, Kopp A, Vacha S, Nuzhdin S, Wayne M. 2004. Extensive sex-specific nonadditivity of gene expression in *Drosophila melanogaster*. *Genetics* 167(4):1791–1799.

Goncalves A, Leigh-Brown S, Thybert D, Stefflova K, Turro E, Flicek P, Brazma A, Odom DT, Marioni JC. 2012. Extensive compensatory *cis–trans* regulation in the evolution of mouse gene expression. *Genome Res.* [Internet] 22(12):2376–2384.

Gorlin RJ, Cohen MM, Hennekam R. 1990. Syndromes of the head and neck. Oxford (UK): Oxford University Press.

Graze RM, McIntyre LM, Main BJ, Wayne ML, Nuzhdin SV. 2009. Regulatory divergence in *Drosophila melanogaster* and *D. simulans*, a genomewide analysis of allele-specific expression. *Genetics* 183(2):547–561.

Griswold CK. 2006. Gene flow's effect on the genetic architecture of a local adaptation and its consequences for QTL analyses. *Heredity (Edinb.) [Internet]* 96(6):445–453.

Gross JB, Powers AK. 2018. A natural animal model system of craniofacial anomalies: the blind Mexican cavefish. *Anat. Rec*. 303:24–29.

Hall BK. 2009. The neural crest and neural crest cells in vertebrate development and evolution. New York: Springer US.

Hart JC, Ellis NA, Eisen MB, Miller CT. 2018. Convergent evolution of gene expression in two high-toothed stickleback populations. *PLoS Genet*. 14(6):e1007443.

Helms JA, Cordero D, Tapadia MD. 2005. New insights into craniofacial morphogenesis. *Development* 132(5):851–861.

Hernandez LP, Adriaens D, Martin CH, Wainwright PC, Masschaele B, Dierick M. 2018. Building trophic specializations that result in substantial niche partitioning within a young adaptive radiation. *J Anat*. 232(2):173–185.

Hindorff LA, Sethupathy P, Junkins HA, Ramos EM, Mehta JP, Collins FS, Manolio TA. 2009. Potential etiologic and functional implications of genome-wide association loci for human diseases and traits. *Proc Natl Acad Sci U S A*. 106(23):9362–9367.

Ho SS, Urban AE, Mills RE. 2019. Structural variation in the sequencing era. *Nat Rev Genet*. 21:171–189.

Huber C, Cormier-Daire V. 2012. Ciliary disorder of the skeleton. *Am J Med Genet*. 160C(3):165–174.

Hughes KA, Ayroles JF, Reedy MM, Drnevich JM, Rowe KC, Ruedi EA, Cáceres CE, Paige KN. 2006. Segregating variation in the transcriptome: cis regulation and additivity of effects. *Genetics* 173(3):1347–1355.

Irwin DE, Alcaide M, Delmore KE, Irwin JH, Owens GL. 2016. Recurrent selection explains parallel evolution of genomic regions of high relative but low absolute differentiation in a ring species. *Mol Ecol*. 25(18):4488–4507.

Jones FC, Grabherr MG, Chan YF, Russell P, Mauceli E, Johnson J, Swofford R, Pirun M, Zody MC, White S, et al. 2012. The genomic basis of adaptive evolution in threespine sticklebacks. *Nature* 484(7392):55–61.

Kessler K, Wunderlich I, Uebe S, Falk NS, Gießl A, Helmut Brandstätter J, Popp B, Klinger P, Ekici AB, Sticht H, et al. 2015. DYNC2LI1 mutations broaden the clinical spectrum of dynein-2 defects. *Sci Rep*. 5:1–12.

Kratochwil CF, Meyer A. 2015. Closing the genotype-phenotype gap: emerging technologies for evolutionary genetics in ecological model vertebrate systems. *BioEssays* 37(2):213–226.

Lamichhaney S, Berglund J, Almén MS, Maqbool K, Grabherr M, Martinez-Barrio A, Promerová M, Rubin C-J, Wang C, Zamani N, et al. 2015. Evolution of Darwin's finches and their beaks revealed by genome sequencing. *Nature [Internet]* 518(7539):371–375.

Landry CR, Hartl DL, Ranz JM. 2007. Genome clashes in hybrids: insights from gene expression. *Heredity (Edinb.)* 99(5):483–493.

Landry CR, Wittkopp PJ, Taubes CH, Ranz JM, Clark AG, Hartl DL. 2005. Compensatory *cis–trans* evolution and the dysregulation of gene expression in interspecific hybrids of *Drosophila*. *Genetics* 171(4):1813–1822.

Lee S, Cook D, Lawrence M. 2019. Plyranges: a grammar of genomic data transformation. *Genome Biol*. 20(1):10.

Lemos B, Araripe LO, Fontanillas P, Hartl DL. 2008. Dominance and the evolutionary accumulation of *cis*- and *trans*-effects on gene expression. *Proc Natl Acad Sci*. 105(38):14471–14476. [Internet]

Lencer ES, McCune AR. 2018. An embryonic staging series up to hatching for *Cyprinodon variegatus*: an emerging fish model for developmental, evolutionary, and ecological research. *J Morphol*. 279(11):1559–1578.

Lencer ES, Warren WC, Harrison R, Mccune AR. 2017. The *Cyprinodon variegatus* genome reveals gene expression changes underlying differences in skull morphology among closely related species. *J Morphol*. 279:1559–1578.

Levin BA, Simonov E, Dgebuadze YY, Levina M, Golubtsov AS. 2020. In the rivers: multiple adaptive radiations of Cyprinid fishes (Labeobarbus) in Ethiopian Highlands. *Sci Rep*. 10:1–13.

Li H, Durbin R. 2011. Inference of human population history from individual whole-genome sequences. *Nature [Internet]* 475(7357):493–496.

Liao Y, Smyth GK, Shi W. 2014. Sequence analysis featureCounts: an efficient general purpose program for assigning sequence reads to genomic features. *Bioinformatics* 30(7):923–930.

Love MI, Huber W, Anders S. 2014. Moderated estimation of fold change and dispersion for RNA-seq data with DESeq2. *Genome Biol*. 15:550.

Mack KL, Campbell P, Nachman MW. 2016. Gene regulation and speciation in house mice. *Genome Res*. 26(4):451–461.

Mack KL, Nachman MW. 2017. Gene regulation and speciation. *Trends Genet.* 33(1):68–80.
Madeira F, Park YM, Lee J, Buso N, Gur T, Madhusoodanan N, Basutkar P, Tivey ARN, Potter SC, Finn RD, et al. 2019. The EMBL-EBI search and sequence analysis tools APIs in 2019. *Nucleic Acids Res.* 47(W1):W636–641.
Martin CH, Erickson PA, Miller CT. 2017. The genetic architecture of novel trophic specialists: larger effect sizes are associated with exceptional oral jaw diversification in a pupfish adaptive radiation. *Mol Ecol.* 26(2):624–638.
Martin CH, Feinstein LC. 2014. Novel trophic niches drive variable progress towards ecological speciation within an adaptive radiation of pupfishes. *Mol Ecol.* 23(7):1846–1862.
Martin CH, McGirr JA, Richards EJ, St. John ME. 2019. How to investigate the origins of novelty: insights gained from genetic, behavioral, and fitness perspectives. *Integr Org Biol.* 1.
Martin CH, Richards EJ. 2019. The paradox behind the pattern of rapid adaptive radiation: how can the speciation process sustain itself through an early burst? *Annu Rev Ecol Evol Syst.* 50(1):1–25.
Martin CH, Wainwright PC. 2011. Trophic novelty is linked to exceptional rates of morphological diversification in two adaptive radiations of *Cyprinodon* pupfish. *Evolution [Internet]* 65(8):2197–2212.
Martin CH, Wainwright PC. 2013a. A remarkable species flock of *Cyprinodon* pupfishes endemic to San Salvador Island, Bahamas. *Bull Peabody Museum Nat Hist. [Internet]* 54(2):231–241.
Martin CH, Wainwright PC. 2013b. Multiple fitness peaks on the adaptive landscape drive adaptive radiation in the wild. *Science [Internet]* 339(6116):208–211.
Martin CH, Wainwright PC. 2013c. On the measurement of ecological novelty: scale-eating pupfish are separated by 168 my from other scale-eating fishes. *PLoS One [Internet]* 8(8):e71164.
Martin SH, Dasmahapatra KK, Nadeau NJ, Salazar C, Walters JR, Simpson F, Blaxter M, Manica A, Mallet J, Jiggins CD. 2013. Genome-wide evidence for speciation with gene flow in *Heliconius* butterflies. *Genome Res.* 23(11):1817–1828.
Maurano MT, Humbert R, Rynes E, Thurman RE, Haugen E, Wang H, Reynolds AP, Sandstrom R, Qu H, Brody J, et al. 2012. Systematic localization of common disease-associated variation in regulatory DNA. *Science (80.)* 337(6099):1190–1195.
Mayba O, Gilbert HN, Liu J, Haverty PM, Jhunjhunwala S, Jiang Z, Watanabe C, Zhang Z. 2014. MBASED: allele-specific expression detection in cancer tissues and cell lines. *Genome Biol.* 15(8):1–21.
McGirr JA, Martin CH. 2017. Novel candidate genes underlying extreme trophic specialization in Caribbean pupfishes. *Mol Biol Evol.* 34(4):873–888.
McGirr JA, Martin CH. 2018. Parallel evolution of gene expression between trophic specialists despite divergent genotypes and morphologies. *Evol Lett.* 2(2):62–75. [Internet]
McGirr JA, Martin CH. 2019. Ecological divergence in sympatry causes gene misregulation in hybrids. *bioRxiv* 717025:1–71.
McManus CJ, Coolon JD, Duff MO, Eipper-Mains J, Graveley BR, Wittkopp PJ. 2010. Regulatory divergence in *Drosophila* revealed by mRNA-seq. *Genome Res.* 20(6):816–825.
Nachman MW, Payseur BA. 2012. Recombination rate variation and speciation: theoretical predictions and empirical results from rabbits and mice. *Phil Trans R Soc B* 367(1587):409–421.
Nguyen D, Xu T. 2008. The expanding role of mouse genetics for understanding human biology and disease. *Dis Model Mech.* 1(1):56–66.
Niceta M, Margiotti K, Digilio MC, Guida V, Bruselles A, Pizzi S, Ferraris A, Memo L, Laforgia N, Dentici ML, et al. 2018. Biallelic mutations in DYNC2LI1 are a rare cause of Ellis-van Creveld syndrome. *Clin Genet.* 93(3):632–639.
Noor MAF, Bennett SM. 2009. Islands of speciation or mirages in the desert? Examining the role of restricted recombination in maintaining species. *Heredity (Edinb).* 103(6):439–444.
Pfister KK, Shah PR, Hummerich H, Russ A, Cotton J, Annuar AA, King SM, Fisher EMC. 2006. Genetic analysis of the cytoplasmic dynein subunit families. *PLoS Genet.* 2(1):e1.
Poelstra JW, Vijay N, Bossu CM, Lantz H, Ryll B, Müller I, Baglione V, Unneberg P, Wikelski M, Grabherr MG, et al. 2014. The genomic landscape underlying phenotypic integrity in the face of gene flow in crows. *Science [Internet]* 344(6190):1410–1414.
Powder KE, Albertson RC. 2016. Cichlid fishes as a model to understand normal and clinical craniofacial variation. *Dev Biol. [Internet]* 415(2):338–346.
Prud'homme B, Gompel N, Carroll SB. 2007. Emerging principles of regulatory evolution. *Proc Natl Acad Sci. [Internet]* 104(Suppl 1):8605–8612.
Rausch T, Zichner T, Schlattl A, Stütz AM, Benes V, Korbel JO. 2012. DELLY: structural variant discovery by integrated paired-end and split-read analysis. *Bioinformatics.* 28:333–339.
Richards EJ, Martin CH. 2017. Adaptive introgression from distant Caribbean islands contributed to the diversification of a microendemic adaptive radiation of trophic specialist pupfishes. *PLoS Genet.* 13(8):e1006919.
Richards AEJ, Mcgirr JA, Wang JR, John MES. 2020. Major stages of vertebrate adaptive radiation are assembled from a disparate spatiotemporal landscape. unpublished, BioRxiv doi.org/10.1101/2020.03.12.988774.
Roberts RB, Hu Y, Albertson RC, Kocher TD. 2011. Craniofacial divergence and ongoing adaptation via the hedgehog pathway. *Proc Natl Acad Sci U S A.* 108(32):13194–13199.
Rottscheidt R, Harr B. 2007. Extensive additivity of gene expression differentiates subspecies of the house mouse. *Genetics* 177(3):1553–1567.
Ruiz-Perez VL, Goodship JA. 2009. Ellis-van Creveld syndrome and Weyers acrodental dysostosis are caused by cilia-mediated diminished response to Hedgehog ligands. *Am J Med Genet.* 151C(4):341–351.
Sadkowski T, Jank M, Zwierzchowski L, Oprzą dek J, Motyl T. 2009. Comparison of skeletal muscle transcriptional profiles in dairy and beef breeds bulls. *J Appl Genet.* 50(2):109–123.
Schaefke B, Emerson JJ, Wang TY, Lu MYJ, Hsieh LC, Li WH. 2013. Inheritance of gene expression level and selective constraints on *trans-* and *cis*-regulatory changes in yeast. *Mol Biol Evol.* 30(9):2121–2133.
Schartl M. 2014. Beyond the zebrafish: diverse fish species for modeling human disease. *Dis Model Mech.* 7(2):181–192.
Schaub MA, Boyle AP, Kundaje A, Batzoglou S, Snyder M. 2012. Linking disease associations with regulatory information in the human genome. *Genome Res.* 22(9):1748–1759.
Schilling TF, Kimmel CB. 1994. Segment and cell type lineage restrictions during pharyngeal arch development in the zebrafish embryo. *Development [Internet]* 120:483–494.
Sella G, Barton NH. 2019. Thinking about the evolution of complex traits in the era of genome-wide association studies. *Annu Rev Genom Hum Genet.* 20(1):461–493.
Shi X, Ng DWK, Zhang C, Comai L, Ye W, Jeffrey Chen Z. 2012. *Cis-* and *trans*-regulatory divergence between progenitor species determines gene-expression novelty in Arabidopsis allopolyploids. *Nat Commun. [Internet]* 3:950–959.
Signor SA, Nuzhdin SV. 2018. The evolution of gene expression in *cis* and *trans*. *Trends Genet.* 34:532–544.
Stapley J, Reger J, Feulner PGD, Smadja C, Galindo J, Ekblom R, Bennison C, Ball AD, Beckerman AP, Slate J. 2010. Adaptation genomics: the next generation. *Trends Ecol Evol. [Internet]* 25(12):705–712.
Stetter MG, Thornton K, Ross-Ibarra J. 2018. Genetic architecture and selective sweeps after polygenic adaptation to distant trait optima. *PLoS Genet.* 14(11):e1007794.
St. John ME, Dixon KE, Martin CH. 2020a. Oral shelling within an adaptive radiation of pupfishes: testing the adaptive function of a novel nasal protrusion and behavioural preference. *J Fish Biol.* 1–9.
St. John ME, Holzman R, Martin CH. 2020b. Rapid adaptive evolution of scale-eating kinematics to a novel ecological niche. *J Exp Biol.* jeb.217570.

St. John ME, McGirr JA, Martin CH. 2019. The behavioral origins of novelty: did increased aggression lead to scale-eating in pupfishes? *Behav Ecol*. 30(2):557–569.

Streisfeld MA, Rausher MD. 2009. Altered trans-regulatory control of gene expression in multiple anthocyanin genes contributes to adaptive flower color evolution in *Mimulus aurantiacus*. *Mol Biol Evol*. 26(2):433–444.

Suvorov A, Nolte V, Pandey RV, Franssen SU, Futschik A, Schlötterer C. 2013. Intra-specific regulatory variation in Drosophila pseudoobscura. *PLoS One*. 8(12):e83547.

Taylor SP, Dantas TJ, Duran I, Wu S, Lachman RS, Consortium G, Nelson SF, Cohn DH, Vallee RB, Krakow D. 2015. Mutations in DYNC2LI1 disrupt cilia function and cause short rib polydactyly syndrome. *Nat Commun. [Internet]* 6:1–11.

Tirosh I, Reikhav S, Levy AA, Barkai N. 2009. A yeast hybrid provides insight into the evolution of gene expression regulation. *Science* 324(5927):659–662.

Turner BJ, Duvernell DD, Bunt TM, Barton MG. 2008. Reproductive isolation among endemic pupfishes (Cyprinodon) on San Salvador Island, Bahamas: microsatellite evidence. *Biol J Linn Soc*. 95(3):566–582.

Van De Geijn B, Mcvicker G, Gilad Y, Pritchard JK. 2015. WASP: allele-specific software for robust molecular quantitative trait locus discovery. *Nat Methods* 12(11):1061–1063.

Verta JP, Jones FC. 2019. Predominance of *cis*-regulatory changes in parallel expression divergence of sticklebacks. *eLife* 8:1–30.

Wang L, Wang S, Li W. 2012. RSeQC: quality control of RNA-seq experiments. *Bioinformatics*. 17:1–16.

Wellenreuther M, Mérot C, Berdan E, Bernatchez L. 2019. Going beyond SNPs: the role of structural genomic variants in adaptive evolution and species diversification. *Mol Ecol*. 28(6):1203–1209.

West RJD, Kodric-Brown A. 2015. Mate Choice by both sexes maintains reproductive isolation in a species flock of pupfish (*Cyprinodon* spp.) in the Bahamas. *Ethology* 121(8):793–800.

Williams BB, Tebbutt NC, Buchert M, Putoczki TL, Doggett K, Bao S, Johnstone CN, Masson F, Hollande F, Burgess AW, et al. 2015. Glycoprotein A33 deficiency: a new mouse model of impaired intestinal epithelial barrier function and inflammatory disease. *Dis Model Mech*. 8(8):805–815.

Wittkopp PJ, Haerum BK, Clark AG. 2008. Regulatory changes underlying expression differences within and between Drosophila species. *Nat Genet*. 40(3):346–350.

Wittkopp PJ, Haerum BK, Clark AG. 2004. Evolutionary changes in *cis* and *trans* gene regulation. *Nature* 430(6995):85–88.

Wittkopp PJ, Kalay G. 2012. *Cis*-regulatory elements: molecular mechanisms and evolutionary processes underlying divergence. *Nat Rev Genet*. 13(1):59–69.

Ye J, Coulouris G, Zaretskaya I, Cutcutache I, Rozen S, Madden TL. 2012. Primer-BLAST: a tool to design target-specific primers for polymerase chain reaction. *BMC Bioinformatics*. 13:134.

Yeaman S, Whitlock MC. 2011. The genetic architecture of adaptation under migration-selection balance. *Evolution* 65(7):1897–1911.